

CPTH-S725.0799  
 DFF/340/07/99  
 LPT-ORSAY 99/58  
 ROM2F-99/22  
 hep-th/9907184

# Open Descendants of $Z_2 \times Z_2$ Freely-Acting Orbifolds

I. Antoniadis<sup>a</sup>, G. D'Appollonio<sup>b</sup>, E. Dudas<sup>c</sup> and A. Sagnotti<sup>a,d</sup>

<sup>a</sup> *Centre de Physique Théorique<sup>†</sup>, Ecole Polytechnique, F-91128 Palaiseau*

<sup>b</sup> *Dipartimento di Fisica, Università di Firenze*

*INFN-Sezione di Firenze*

*Largo Enrico Fermi 2, 50125 Firenze ITALY*

<sup>c</sup> *LPT<sup>‡</sup>, Bât. 210, Univ. Paris-Sud, F-91405 Orsay*

<sup>d</sup> *Dipartimento di Fisica, Università di Roma “Tor Vergata”*

*INFN, Sezione di Roma “Tor Vergata”*

*Via della Ricerca Scientifica 1, 00133 Roma ITALY*

## Abstract

We discuss  $Z_2 \times Z_2$  orientifolds where the orbifold twists are accompanied by shifts on momentum or winding lattice states. The models contain variable numbers of D5 branes, whose massless (and, at times, even massive) modes have variable numbers of supersymmetries. We display new type-I models with partial supersymmetry breaking  $N = 2 \rightarrow N = 1$ ,  $N = 4 \rightarrow N = 1$  and  $N = 4 \rightarrow N = 2$ . The geometry of these models is rather rich: the shift operations create brane multiplets related by orbifold transformations that support gauge groups of reduced rank. Some of the models are deformations of six-dimensional supersymmetric type-I models, while others have dual M-theory descriptions.

---

<sup>\*</sup>Research supported in part by the EEC under TMR contract ERBFMRX-CT96-0090.

<sup>†</sup>CNRS-UMR-7644.

<sup>‡</sup>Laboratoire associé au CNRS-URA-D0063.

## 1. Introduction

Freely acting orbifolds are a useful tool for connecting string vacua with different numbers of supersymmetries. The resulting models provide string realizations of the Scherk-Schwarz mechanism [1, 2, 3], where additional supersymmetries may be recovered in an appropriate decompactification limit. If the original model has extended supersymmetry, the corresponding BPS states, still present in the vacuum with lower supersymmetry, have mass shifts determined by the spontaneous breaking. As a result, duality relations generally continue to hold by the adiabatic argument, and the dynamics of the new vacua simplifies greatly [4].

Type I models may be directly linked [5] to models of oriented closed strings, and in particular to those considered in [3]. They allow an interesting new possibility compared to the heterotic and type II models studied previously [6, 7]: branes orthogonal to the coordinate used for the breaking have full supersymmetry for their massless excitations at tree level, and feel the breaking only through radiative corrections. This phenomenon, generically non-perturbative on the heterotic side, is of some interest in the current literature on brane Kaluza-Klein scenarios, where it is usually referred to as “brane supersymmetry” [8]. From a more technical perspective, the closed sector of these models involves asymmetric projections, so that the construction of the open descendants presents some peculiar features. Asymmetric models have recently been studied in a different context, since they provide an interesting route toward a small or vanishing cosmological constant [9]. The corresponding open descendants, studied in [10], display an even more peculiar feature: all massive brane modes, not only the massless ones, can have an extended supersymmetry [8].

In this work we provide new examples of this class of models in the context of  $Z_2 \times Z_2$  orbifolds where the conventional projections are accompanied by  $Z_2$ -valued momentum or winding lattice shifts. Their open descendants exhibit  $N = 4 \rightarrow N = 1$  or  $N = 2 \rightarrow N = 1$

partial supersymmetry breaking, and involve interesting D-brane configurations, with a rich geometrical structure, that we describe in some detail. These models display enhanced supersymmetry for the massless modes on the branes, and in some cases also for their massive excitations, as the asymmetric orbifolds discussed in [10]. The presence of extended supersymmetry in some of the branes, however, has a drawback in the present construction, since the models we exhibit here are not chiral.

An important new feature is that the branes typically arrange themselves in multiplets of images that are interchanged by some of the orbifold operations. The components of a multiplet share the corresponding Chan-Paton charges and, as a result, the rank of the corresponding gauge groups is reduced, as in models with a quantized NS antisymmetric tensor [11]. Here the displacement of branes that results in the creation of the multiplets is generally unavoidable, so that even the most symmetric configuration typically involves several images. Moreover, the image branes play a crucial role in the local tadpole cancellation along the (shifted) directions transverse to the branes. More precisely, as we will discuss in detail in explicit models, a doublet of image branes ensures the local cancellation of tadpoles introduced in one transverse direction by its two orientifold plane charges, while a quadruplet of image branes ensures local tadpole cancellation in two transverse (shifted) directions. These conditions are effective if the various types of branes do not intersect, a property shared by all our configurations. As a result, in most of our models the local tadpole conditions are automatically satisfied, thanks to the images that appear since the branes are generally forced away from their fixed points. Other brane configurations with less supersymmetry are also possible, but they do not satisfy local tadpole cancellation. Compared with toroidal examples, where local tadpoles require that the gauge group, of rank 16, be broken by Wilson lines [14] , in our examples a set of  $m$  image branes share the same gauge group that, however, has a rank reduced to  $16/m$ .

This paper is organized as follows. In Section 2 we describe the structure of the su-

persymmetric  $Z_2 \times Z_2$  model without discrete torsion<sup>1</sup>. In Section 3 we define the “shift orientifolds” and describe qualitatively their main properties, the structure of the corresponding D-brane configurations and identify various instances of brane supersymmetry. In Section 4 we present the conformal field theory description and the open string partition functions for branes away from fixed points in simple examples, while in Section 5 we describe a model with  $N = 2 \rightarrow N = 1$  breaking that displays rather clearly all the salient features of our constructions. Section 6, 7 and 8 contain a description of models with two, one and zero sets of D5 branes, including their limiting behaviors for large or small radii where extended supersymmetry is recovered, and their relation to M-theory compactifications. Finally, Section 9 contains the summary of our results and our conclusions.

## 2. Supersymmetric $Z_2 \times Z_2$ models

There are two classes of supersymmetric  $Z_2 \times Z_2$  models, that differ from one another because of the presence of “discrete torsion” [13]. In the partition function, this is a sign associated to an independent modular orbit, with crucial effects both on the massless field content and on the structure of the descendants. These orbifolds are singular limits of Calabi-Yau spaces, with Hodge numbers  $(3, 51)$  and  $(51, 3)$  respectively.

The torus amplitudes for the supersymmetric  $Z_2 \times Z_2$  models are

$$\begin{aligned}
 \mathcal{T} = & \frac{1}{4} \left\{ |T_{oo}|^2 \Lambda_1 \Lambda_2 \Lambda_3 + |T_{og}|^2 \Lambda_1 \left| \frac{4\eta^2}{\theta_2^2} \right|^2 + |T_{oh}|^2 \Lambda_3 \left| \frac{4\eta^2}{\theta_2^2} \right|^2 + |T_{of}|^2 \Lambda_2 \left| \frac{4\eta^2}{\theta_2^2} \right|^2 \right. \\
 & + |T_{go}|^2 \Lambda_1 \left| \frac{4\eta^2}{\theta_4^2} \right|^2 + |T_{gg}|^2 \Lambda_1 \left| \frac{4\eta^2}{\theta_3^2} \right|^2 + |T_{ho}|^2 \Lambda_3 \left| \frac{4\eta^2}{\theta_4^2} \right|^2 + |T_{hh}|^2 \Lambda_3 \left| \frac{4\eta^2}{\theta_3^2} \right|^2 \\
 & + |T_{fo}|^2 \Lambda_2 \left| \frac{4\eta^2}{\theta_4^2} \right|^2 + |T_{ff}|^2 \Lambda_2 \left| \frac{4\eta^2}{\theta_3^2} \right|^2 \\
 & \left. + \epsilon \left( |T_{gh}|^2 + |T_{gf}|^2 + |T_{fg}|^2 + |T_{fh}|^2 + |T_{hg}|^2 + |T_{hf}|^2 \right) \left| \frac{8\eta^3}{\theta_2 \theta_3 \theta_4} \right|^2 \right\} , \quad (2.1)
 \end{aligned}$$

---

<sup>1</sup>Discrete torsion introduces peculiar new features in the open descendants, and will be discussed elsewhere [12].

where  $\Lambda_1$ ,  $\Lambda_2$  and  $\Lambda_3$  denote the three lattice sums associated to the three internal tori  $T_{45}$ ,  $T_{67}$  and  $T_{89}$  of the compactification and  $\epsilon = \pm 1$ . Here, as in all following amplitudes, we are leaving the contributions of transverse bosons implicit. The choice  $\epsilon = 1$  defines the model without discrete torsion, while the choice  $\epsilon = -1$  defines the model with discrete torsion. The model with discrete torsion is quite interesting, since its descendants contain chiral fermions, but presents some difficulties, since some of the “untwisted” tadpoles can not be eliminated in the usual way, and will be discussed elsewhere.

As usual, the arguments depend on  $q = \exp(2\pi i\tau)$  and its conjugate, where  $\tau$  is the modulus of the torus. For later convenience, we have expressed the torus amplitude in terms of the 16 quantities  $T_{ij}$  ( $i = o, g, h, f$ ):

$$\begin{aligned} T_{io} &= \tau_{io} + \tau_{ig} + \tau_{ih} + \tau_{if} \quad , & T_{ig} &= \tau_{io} + \tau_{ig} - \tau_{ih} - \tau_{if} \quad , \\ T_{ih} &= \tau_{io} - \tau_{ig} + \tau_{ih} - \tau_{if} \quad , & T_{if} &= \tau_{io} - \tau_{ig} - \tau_{ih} + \tau_{if} \quad , \end{aligned} \quad (2.2)$$

where the 16  $Z_2 \times Z_2$  characters  $\tau_{ij}$  are [16]

$$\begin{aligned} \tau_{oo} &= V_2 O_2 O_2 O_2 + O_2 V_2 V_2 V_2 - S_2 S_2 S_2 S_2 - C_2 C_2 C_2 C_2 \ , \\ \tau_{og} &= O_2 V_2 O_2 O_2 + V_2 O_2 V_2 V_2 - C_2 C_2 S_2 S_2 - S_2 S_2 C_2 C_2 \ , \\ \tau_{oh} &= O_2 O_2 O_2 V_2 + V_2 V_2 V_2 O_2 - C_2 S_2 S_2 C_2 - S_2 C_2 C_2 S_2 \ , \\ \tau_{of} &= O_2 O_2 V_2 O_2 + V_2 V_2 O_2 V_2 - C_2 S_2 C_2 S_2 - S_2 C_2 S_2 C_2 \ , \\ \tau_{go} &= V_2 O_2 S_2 C_2 + O_2 V_2 C_2 S_2 - S_2 S_2 V_2 O_2 - C_2 C_2 O_2 V_2 \ , \\ \tau_{gg} &= O_2 V_2 S_2 C_2 + V_2 O_2 C_2 S_2 - S_2 S_2 O_2 V_2 - C_2 C_2 V_2 O_2 \ , \\ \tau_{gh} &= O_2 O_2 S_2 S_2 + V_2 V_2 C_2 C_2 - C_2 S_2 V_2 V_2 - S_2 C_2 O_2 O_2 \ , \\ \tau_{gf} &= O_2 O_2 C_2 C_2 + V_2 V_2 S_2 S_2 - S_2 C_2 V_2 V_2 - C_2 S_2 O_2 O_2 \ , \\ \tau_{ho} &= V_2 S_2 C_2 O_2 + O_2 C_2 S_2 V_2 - C_2 O_2 V_2 C_2 - S_2 V_2 O_2 S_2 \ , \\ \tau_{hg} &= O_2 C_2 C_2 O_2 + V_2 S_2 S_2 V_2 - C_2 O_2 O_2 S_2 - S_2 V_2 V_2 C_2 \ , \end{aligned}$$

$$\begin{aligned}
\tau_{hh} &= O_2 S_2 C_2 V_2 + V_2 C_2 S_2 O_2 - S_2 O_2 V_2 S_2 - C_2 V_2 O_2 C_2 , \\
\tau_{hf} &= O_2 S_2 S_2 O_2 + V_2 C_2 C_2 V_2 - C_2 V_2 V_2 S_2 - S_2 O_2 O_2 C_2 , \\
\tau_{fo} &= V_2 S_2 O_2 C_2 + O_2 C_2 V_2 S_2 - S_2 V_2 S_2 O_2 - C_2 O_2 C_2 V_2 , \\
\tau_{fg} &= O_2 C_2 O_2 C_2 + V_2 S_2 V_2 S_2 - C_2 O_2 S_2 O_2 - S_2 V_2 C_2 V_2 , \\
\tau_{fh} &= O_2 S_2 O_2 S_2 + V_2 C_2 V_2 C_2 - C_2 V_2 S_2 V_2 - S_2 O_2 C_2 O_2 , \\
\tau_{ff} &= O_2 S_2 V_2 C_2 + V_2 C_2 O_2 S_2 - C_2 V_2 C_2 O_2 - S_2 O_2 S_2 V_2 , \tag{2.3}
\end{aligned}$$

with  $O_2, V_2, S_2, C_2$  the four  $O(2)$  level-one characters. The ordering of the four factors refers to the eight transverse dimensions of space time and, in particular, the first factor is associated to the two transverse space-time directions. The notation  $(o, g, h, f)$  reflects the four operations in  $Z_2 \times Z_2$ . Aside from the identity  $o$ , these act as  $\pi$ -rotations on two of the three internal tori, namely

$$g : (+, -, -) \quad , \quad f : (-, +, -) \quad , \quad h : (-, -, +) \quad . \tag{2.4}$$

One can now follow the usual procedure and build the three additional amplitudes that, together with (2.1), determine the spectrum of the open descendants: Klein-bottle  $\mathcal{K}$ , annulus  $\mathcal{A}$  and Möbius strip  $\mathcal{M}$ . There are actually a number of distinct choices for  $\mathcal{K}$ , that correspond to different choices for three signs  $(\epsilon_1, \epsilon_2, \epsilon_3)$  that define the worldsheet projection for twisted states. In all cases these signs are related to the parameter  $\epsilon$  introduced previously, since they must satisfy

$$\epsilon_1 \epsilon_2 \epsilon_3 = \epsilon \quad . \tag{2.5}$$

Thus, the models with discrete torsion require an *odd* number of negative signs, while the models without discrete torsion require an *even* number of negative signs. Let us now introduce the restrictions of the full lattice sums  $\Lambda_i$  to their momentum and winding sub-lattices. These will be denoted by  $P_i$  and  $W_i$ , where the index identifies the corresponding

two-torus. In later Sections, as in [6, 7], we shall also need sums with alternating signs in one direction of the two-tori, that we shall denote succinctly as  $(-1)^m P$  or  $(-1)^n W$ . In terms of these quantities the Klein-bottle amplitude in the direct channel is

$$\begin{aligned} \mathcal{K} = & \frac{1}{8} \left\{ (P_1 P_2 P_3 + P_1 W_2 W_3 + W_1 P_2 W_3 + W_1 W_2 P_3) T_{oo} \right. \\ & \left. + 2 \times 16 [\epsilon_1 (P_1 + \epsilon W_1) T_{go} + \epsilon_2 (P_2 + \epsilon W_2) T_{fo} + \epsilon_3 (P_3 + \epsilon W_3) T_{ho}] \left( \frac{\eta}{\theta_4} \right)^2 \right\} \quad (2.6) \end{aligned}$$

The discrete torsion has a crucial effect on this term. Indeed, while for  $\epsilon = 1$  the massless twisted contributions are diagonal combinations of the  $\tau$ 's, and describe  $N = 2$  vector multiplets, for  $\epsilon = -1$  they are off-diagonal ones that describe (chiral-linear) hypermultiplets, and therefore do not contribute to the Klein bottle amplitude. This feature reflects itself in the nature of the terms  $(P_i + \epsilon W_i)$  in  $\mathcal{K}$ . While for  $\epsilon = -1$  these have no massless contributions, for  $\epsilon = +1$  they do, and one has additional options, related to the  $\epsilon_i$ . For instance, starting from the original twisted  $N = 2$  vector multiplets, in the Klein-bottle projection  $\epsilon_1 = 1$  selects  $N = 1$  chiral multiplets, while  $\epsilon_1 = -1$  selects vector multiplets.

An  $S$  transformation turns this expression into the corresponding vacuum-channel amplitude

$$\begin{aligned} \tilde{\mathcal{K}} = & \frac{2^5}{8} \left\{ (v_1 v_2 v_3 W_1^e W_2^e W_3^e + \frac{v_1}{v_2 v_3} W_1^e P_2^e P_3^e + \frac{v_2}{v_1 v_3} P_1^e W_2^e P_3^e + \frac{v_3}{v_1 v_2} P_1^e P_2^e W_3^e) T_{oo} \right. \\ & \left. + 2 [\epsilon_1 (v_1 W_1^e + \epsilon \frac{P_1^e}{v_1}) T_{og} + \epsilon_2 (v_2 W_2^e + \epsilon \frac{P_2^e}{v_2}) T_{of} + \epsilon_3 (v_3 W_3^e + \epsilon \frac{P_3^e}{v_3}) T_{oh}] \left( \frac{2\eta}{\theta_2} \right)^2 \right\}, \quad (2.7) \end{aligned}$$

where the superscript  $e$  stands for the usual restriction of the lattice terms to their even subsets. The structure of this term relates the three signs  $\epsilon_i$  to the discrete torsion  $\epsilon = \pm 1$ . This is neatly displayed by confining the attention to the terms at the origin of the lattices, that are to group into perfect squares. Indeed, the corresponding amplitude,

$$\begin{aligned} \tilde{\mathcal{K}}_0 = & \frac{2^5}{8} \left\{ \left( \sqrt{v_1 v_2 v_3} + \epsilon_1 \sqrt{\frac{v_1}{v_2 v_3}} + \epsilon_2 \sqrt{\frac{v_2}{v_1 v_3}} + \epsilon_3 \sqrt{\frac{v_3}{v_1 v_2}} \right)^2 \tau_{oo} \right. \\ & \left. + \left( \sqrt{v_1 v_2 v_3} + \epsilon_1 \sqrt{\frac{v_1}{v_2 v_3}} - \epsilon_2 \sqrt{\frac{v_2}{v_1 v_3}} - \epsilon_3 \sqrt{\frac{v_3}{v_1 v_2}} \right)^2 \tau_{og} \right\} \end{aligned}$$

$$\begin{aligned}
 & + \left( \sqrt{v_1 v_2 v_3} - \epsilon_1 \sqrt{\frac{v_1}{v_2 v_3}} + \epsilon_2 \sqrt{\frac{v_2}{v_1 v_3}} - \epsilon_3 \sqrt{\frac{v_3}{v_1 v_2}} \right)^2 \tau_{of} \\
 & + \left( \sqrt{v_1 v_2 v_3} - \epsilon_1 \sqrt{\frac{v_1}{v_2 v_3}} - \epsilon_2 \sqrt{\frac{v_2}{v_1 v_3}} + \epsilon_3 \sqrt{\frac{v_3}{v_1 v_2}} \right)^2 \tau_{oh} \}
 \end{aligned} \tag{2.8}$$

displays four independent squared reflection coefficients, related to the 9-brane and to the three types of 5-branes, *only* if eq. (2.5) is satisfied. It should be appreciated that the constraint (2.5) implies that, in the presence of discrete torsion, at least one of the orientifold charges is reversed. This is the problem we mentioned at the beginning. Here we confine our attention to the choice  $\epsilon_1 = \epsilon_2 = \epsilon_3 = 1$  for the model without discrete torsion.

It is instructive to review the structure of the open descendants for the model without discrete torsion. The orbifold breakings are not allowed in this case: the twisted terms involve diagonal combinations of the (non-self-conjugate) characters  $\tau_{ij}$ , that cannot flow in the tube channel. The allowed terms describe the familiar  $NN$ ,  $ND$  and  $DD$  strings or, in brane language, the  $99$ ,  $5_i 9$  and  $5_i 5_j$  terms, together with additional, more peculiar,  $5_i 5_j$  strings. For the sake of simplicity, let us also refrain from introducing Wilson lines, insert all 5-branes at the origin and exclude a quantized  $NS$   $B_{ab}$ , in order to obtain a relatively simple model with a maximal gauge group.

The annulus amplitude for the model without discrete torsion is

$$\begin{aligned}
 \mathcal{A} = & \frac{1}{8} \left\{ (N^2 P_1 P_2 P_3 + D_1^2 P_1 W_2 W_3 + D_2^2 W_1 P_2 W_3 + D_3^2 W_1 W_2 P_3) T_{oo} \right. \\
 & + 2(N D_1 P_1 T_{go} + N D_2 P_2 T_{fo} + N D_3 P_3 T_{ho}) \left( \frac{\eta}{\theta_4} \right)^2 \\
 & \left. + 2(D_2 D_3 W_1 T_{go} + D_1 D_3 W_2 T_{fo} + D_1 D_2 W_3 T_{ho}) \left( \frac{\eta}{\theta_4} \right)^2 \right\} .
 \end{aligned} \tag{2.9}$$

Aside from the standard  $NN$  terms associated with the 9-branes, there are indeed three types of standard  $D_i^2$  terms, and corresponding  $N D_i$  terms. Each of these  $D_i D_i$  strings, however, is only confined within one of the three two-tori, but is free to move at will on it. In addition, there are three other types of strings of a more peculiar nature, where Dirichlet

and Neumann conditions are entangled. The need for all these types of strings can easily be appreciated by noticing that, relatively to the three internal two-tori, the three twists of the  $Z_2 \times Z_2$  orbifold result in open string ends with boundary conditions of four types:  $NNN$ ,  $NDD$ ,  $DND$  and  $DDN$ . Combining these boundaries in all possible ways yields all types of open strings present in the model. Aside from the familiar  $NN$ ,  $ND_i$  and  $D_iD_i$  strings, the spectrum thus includes three additional types of open strings, that are  $DD$  with respect to a torus and  $ND$  with respect to the others. For instance, the combination of  $NDD$  and  $DND$  is a string of this type,  $DD$  in the third torus and  $ND$  in the first two.

An  $S$  transformation turns (2.9) into the corresponding vacuum-channel amplitude

$$\begin{aligned} \tilde{\mathcal{A}} = & \frac{2^{-5}}{8} \left\{ (N^2 v_1 v_2 v_3 W_1 W_2 W_3 + \frac{D_1^2 v_1}{v_2 v_3} W_1 P_2 P_3 + \frac{D_2^2 v_2}{v_1 v_3} P_1 W_2 P_3 + \frac{D_3^2 v_3}{v_1 v_2} P_1 P_2 W_3) T_{oo} \right. \\ & + 2(ND_1 v_1 W_1 T_{og} + ND_2 v_2 W_2 T_{of} + ND_3 v_3 W_3 T_{oh}) \left( \frac{2\eta}{\theta_2} \right)^2 \\ & \left. + 2(D_2 D_3 \frac{1}{v_1} P_1 T_{og} + D_1 D_3 \frac{1}{v_2} P_2 T_{of} + D_1 D_2 \frac{1}{v_3} P_3 T_{oh}) \left( \frac{2\eta}{\theta_2} \right)^2 \right\} , \end{aligned} \quad (2.10)$$

whose neat structure can be exhibited confining the attention to the terms at the origin of the lattice sums, that as usual rearrange themselves into perfect squares. Indeed,

$$\begin{aligned} \tilde{\mathcal{A}}_0 = & \frac{2^{-5}}{8} \left\{ (N\sqrt{v_1 v_2 v_3} + D_1\sqrt{\frac{v_1}{v_2 v_3}} + D_2\sqrt{\frac{v_2}{v_1 v_3}} + D_3\sqrt{\frac{v_3}{v_1 v_2}})^2 \tau_{oo} \right. \\ & + (N\sqrt{v_1 v_2 v_3} + D_1\sqrt{\frac{v_1}{v_2 v_3}} - D_2\sqrt{\frac{v_2}{v_1 v_3}} - D_3\sqrt{\frac{v_3}{v_1 v_2}})^2 \tau_{og} \\ & + (N\sqrt{v_1 v_2 v_3} - D_1\sqrt{\frac{v_1}{v_2 v_3}} + D_2\sqrt{\frac{v_2}{v_1 v_3}} - D_3\sqrt{\frac{v_3}{v_1 v_2}})^2 \tau_{of} \\ & \left. + (N\sqrt{v_1 v_2 v_3} - D_1\sqrt{\frac{v_1}{v_2 v_3}} - D_2\sqrt{\frac{v_2}{v_1 v_3}} + D_3\sqrt{\frac{v_3}{v_1 v_2}})^2 \tau_{oh} \right\} \end{aligned} \quad (2.11)$$

displays four independent squared reflection coefficients, related to the 9-branes and to the three types of 5-branes, and all terms enter this expression with signs fixed by the relation between spin and statistics for the open spectrum in  $\mathcal{A}$ .

These amplitudes determine by standard methods the vacuum channel of the Möbius

amplitude at the origin of the lattices

$$\begin{aligned}
 \tilde{\mathcal{M}}_0 = & -\frac{1}{4} \left\{ [Nv_1v_2v_3 + D_1\frac{v_1}{v_2v_3} + D_2\frac{v_2}{v_1v_3} + D_3\frac{v_3}{v_1v_2}] \hat{T}_{oo} \right. \\
 & + [(N+D_1)v_1 + (D_3+D_2)\frac{1}{v_1}] \hat{T}_{og} + [(N+D_2)v_2 + (D_3+D_1)\frac{1}{v_2}] \hat{T}_{of} \\
 & \left. + [(N+D_3)v_3 + (D_2+D_1)\frac{1}{v_3}] \hat{T}_{oh} \right\} . \quad (2.12)
 \end{aligned}$$

Here, this and all other Möbius amplitudes are expressed in terms of a convenient real basis of “hatted” characters. These may be defined starting from

$$\chi(q) = q^{h-c/24} \sum_n d_n q^n , \quad (2.13)$$

letting  $q \rightarrow e^{i\pi}q$  and removing an overall phase, so that

$$\hat{\chi}(q) = q^{h-c/24} \sum_n (-1)^n d_n q^n . \quad (2.14)$$

For the hatted characters, the modular transformation connecting direct and transverse Möbius channels is  $P = T^{1/2}ST^2ST^{1/2}$ , where  $T : \tau \rightarrow \tau + 1$  and  $S : \tau \rightarrow -1/\tau$ . The whole  $\tilde{\mathcal{M}}$  is then

$$\begin{aligned}
 \tilde{\mathcal{M}} = & -\frac{1}{4} \left\{ [Nv_1v_2v_3W_1^eW_2^eW_3^e + \frac{D_1v_1}{v_2v_3}W_1^eP_2^eP_3^e + \frac{D_2v_2}{v_1v_3}P_1^eW_2^eP_3^e + \frac{D_3v_3}{v_1v_2}P_1^eP_2^eW_3^e] \hat{T}_{oo} \right. \\
 & + [(N+D_1)v_1W_1^e + (D_3+D_2)\frac{P_1^e}{v_1}] \hat{T}_{og} \left( \frac{2\hat{\eta}}{\hat{\theta}_2} \right)^2 + [(N+D_2)v_2W_2^e + (D_3+D_1)\frac{P_2^e}{v_2}] \hat{T}_{of} \left( \frac{2\hat{\eta}}{\hat{\theta}_2} \right)^2 \\
 & \left. + [(N+D_3)v_3W_3^e + (D_2+D_1)\frac{P_3^e}{v_3}] \hat{T}_{oh} \left( \frac{2\hat{\eta}}{\hat{\theta}_2} \right)^2 \right\} , \quad (2.15)
 \end{aligned}$$

and a  $P$  transformation recovers the direct-channel Möbius amplitude

$$\begin{aligned}
 \mathcal{M} = & -\frac{1}{8} \left\{ [NP_1P_2P_3 + D_1P_1W_2W_3 + D_2W_1P_2P_3 + D_3W_1W_2P_3] \hat{T}_{oo} \right. \\
 & - [(N+D_1)P_1 + (D_3+D_2)W_1] \hat{T}_{og} \left( \frac{2\hat{\eta}}{\hat{\theta}_2} \right)^2 - [(N+D_2)P_2 + (D_3+D_1)W_2] \hat{T}_{of} \left( \frac{2\hat{\eta}}{\hat{\theta}_2} \right)^2 \\
 & \left. - [(N+D_3)P_3 + (D_2+D_1)W_3] \hat{T}_{oh} \left( \frac{2\hat{\eta}}{\hat{\theta}_2} \right)^2 \right\} . \quad (2.16)
 \end{aligned}$$

The terms at the origin in (2.8), (2.11) and (2.12) combine, by construction, into the perfect squares of the (untwisted) tadpole conditions

$$N = D_1 = D_2 = D_3 = 32 \quad . \quad (2.17)$$

Notice that the Möbius amplitude reveals the presence of four symplectic gauge groups. The lack of breaking terms, however, requires a rescaling of the four charges by a factor two, in order to grant a proper particle interpretation, and the resulting gauge group is  $USp(16)^4$ . This model was discussed in [15] and, at a rational point, was previously considered in [16].

The massless spectrum can be easily read from  $\mathcal{A}$  and  $\mathcal{M}$ . It is clearly not chiral, and is thus free of gauge and gravitational anomalies. Rescaling the charges, so that  $N = 2n$  and  $D_i = 2d_i$ , one obtains

$$\begin{aligned} \mathcal{A}_0 &= \frac{n^2 + d_1^2 + d_2^2 + d_3^2}{2} (\tau_{oo} + \tau_{og} + \tau_{oh} + \tau_{of}) + (nd_1 + d_2 d_3) (\tau_{go} + \tau_{gg} + \tau_{gh} + \tau_{gf}) \\ &\quad + (nd_2 + d_1 d_3) (\tau_{fo} + \tau_{fg} + \tau_{fh} + \tau_{ff}) + (nd_3 + d_1 d_2) (\tau_{ho} + \tau_{hg} + \tau_{hh} + \tau_{hf}) \quad , \end{aligned} \quad (2.18)$$

$$\mathcal{M}_0 = \frac{1}{2} (n + d_1 + d_2 + d_3) (\tau_{oo} - \tau_{og} - \tau_{of} - \tau_{oh}) \quad . \quad (2.19)$$

These amplitudes describe the adjoint vector multiplets of the four  $USp(16)$  groups, three chiral multiplets, each in the  $(120, 1, 1, 1)$ ,  $(1, 120, 1, 1)$ ,  $(1, 1, 120, 1)$  and  $(1, 1, 1, 120)$ , and six chiral multiplets in the  $(16, 16, 1, 1)$  and in five additional bi-fundamental representations that differ by permutations of the factors.

### 3. General properties of $Z_2 \times Z_2$ shift orientifolds

If conventional orbifold operations are combined with shifts  $(\delta_L, \delta_R)$ , the resulting models provide string realizations [3] of the Scherk-Schwarz mechanism [1]. In this Section we would like to describe the salient features of the combined effects of shifts  $(\delta_L, \delta_R)$  and  $Z_2 \times Z_2$  orbifold operations on the open descendants of type-IIB compactifications. As in

[6, 7], we shall distinguish between symmetric *momentum* shifts  $(p) = (\delta, \delta)$  and antisymmetric *winding* shifts  $(w) = (\delta, -\delta)$ , since the two have very different effects on the resulting spectra. These orbifolds correspond to singular limits of Calabi-Yau manifolds with Hodge numbers  $(19, 19)$ ,  $(11, 11)$  and  $(3, 3)$  in the cases of one, two and three shifts respectively.

Let us begin by introducing a convenient notation to specify the orbifold action  $X_i \rightarrow \sigma(X_i)$  on the complex coordinates for the three internal tori. There are several ways to combine the three operations  $g$ ,  $f$  and  $h$  of eq. (2.4) with shifts in a way consistent with the  $Z_2 \times Z_2$  group structure. However, up to T-dualities and corresponding redefinitions of the  $\Omega$  projection, all non-trivial possibilities are captured by

$$\sigma_1(\delta_1, \delta_2, \delta_3) = \begin{pmatrix} \delta_1 & -\delta_2 & -1 \\ -1 & \delta_2 & -\delta_3 \\ -\delta_1 & -1 & \delta_3 \end{pmatrix}, \quad \sigma_2(\delta_1, \delta_2, \delta_3) = \begin{pmatrix} \delta_1 & -1 & -1 \\ -1 & \delta_2 & -\delta_3 \\ -\delta_1 & -\delta_2 & \delta_3 \end{pmatrix}, \quad (3.1)$$

where the three lines refer to the new operations, that we shall continue to denote by  $g$ ,  $h$  and  $f$ , and where  $-\delta_i$  indicates the combination of a shift in the direction  $i$  with an orbifold inversion. It is simple to convince oneself that the two matrices  $\sigma_1$  and  $\sigma_2$  essentially exhaust all interesting possibilities within this class of models. In order to reach this conclusion, it is important to recognize that when a shift only occurs in combination with an orbifold inversion, it corresponds to a mere rotation of the fixed points, up to T-dualities and redefinitions of the  $\Omega$  projection. Models of this type are *not* freely-acting orbifolds, but rather conventional  $Z_2 \times Z_2$  orbifolds with unconventional  $\Omega$  projections, and therefore are not discussed in this paper, although in some cases they lead to interesting chiral spectra. For instance, a similar winding shift eliminates some branes and yields chiral open descendants. Another possibility, not considered here, is to combine the  $\Omega$  projection with only one of the two group elements of  $Z_2 \times Z_2$ .

T-duality transformations can be neatly discussed referring to the tables (3.1), if these are supplemented by an additional line corresponding to the identity operation. A T-duality along a torus simply flips the signs in the corresponding column and interchanges

momentum and winding shifts. For instance, starting from  $\sigma_1$  and performing a T-duality along  $T_{67}$  and  $T_{89}$  would result in the table

$$\begin{pmatrix} 1 & -1 & -1 \\ \delta_1 & \delta'_2 & 1 \\ -1 & -\delta'_2 & \delta'_3 \\ -\delta_1 & 1 & -\delta'_3 \end{pmatrix} , \quad (3.2)$$

where  $\delta'$  denotes a dual shift. This is equivalent to a standard table  $\sigma_1(\delta_1, \delta'_2, \delta'_3)$ , up to a redefinition of  $\Omega$ , that now includes a factor  $(-1)^{\delta_1 + \delta'_2}$ .

In the following, we shall display a set of independent models, corresponding to various choices of momentum and winding shifts, while restricting our attention to a conventional  $\Omega$  projection. Other choices for  $\Omega$ , including shifts, may be similarly discussed. As in [18, 19], they generally affect the brane content, removing (or even adding) branes. With this proviso, we can confine our attention to ten different types of  $Z_2 \times Z_2$  shift orbifolds.

A simple and general rule predicts the types of allowed branes, and will be justified in the following Sections:

*When a line of the table contains  $p$  or  $-w$ , the corresponding brane is eliminated.*

On the other hand, our choice of referring to a conventional  $\Omega$  projection will always result in leaving the  $D9$  branes unaffected. Up to T-dualities and redefinitions of  $\Omega$ , one can then show that all interesting brane configurations may be captured referring to the ten different models of Table 1.

5-Branes	$\sigma_1$	$\sigma_2$
0	$p_{123}$ $w_{123}$	$p_1 w_2 w_3$
1	$w_1 p_2 w_3$	$w_1 p_2 p_3$ $w_1 p_2$ $p_{23}$
2	$p_3$	$w_2 p_3$ $w_1 w_2 p_3$

Table 1. Types of shift models.

In listing these models, we have made suitable choices of axes, so that when a single  $D5$  brane is present, this is always the first,  $D5_1$ , and when two are present, these are always  $D5_1$  and  $D5_2$ . All these models have  $N = 1$  supersymmetry in the closed sector, but present interesting instances of “brane supersymmetry” [6, 8]: additional supersymmetries are present for the massless modes, and at times also for the massive ones [10], confined to some branes. It is therefore interesting to display, for all the models of Table 1, the number of supersymmetries of the massless modes for the various branes present. The results are summarized in table 2:

models	$D9$ susy	$D5_1$ susy	$D5_2$ susy
$p_3$	N=1	N=2	N=2
$w_2p_3$	N=2	N=2	N=4
$w_1w_2p_3$	N=4	N=4	N=4
$p_{23}$	N=1	N=2	–
$w_1p_2$	N=2	N=4	–
$w_1p_2p_3$	N=2	N=4	–
$w_1p_2w_3$	N=4	N=4	–
$p_{123}$	N=1	–	–
$p_1w_2w_3$	N=2	–	–
$w_1w_2w_3$	N=4	–	–

Table 2. Brane supersymmetry for the various models.

Since the  $p_{123}$  case was already discussed in [7], in the following we can confine our attention to the nine remaining classes of models.

In all models with one or two shifts, the supersymmetry enhancement for the massless modes on the branes may be traced directly to the phenomenon described in [6, 7]: projections accompanied by momentum shifts orthogonal to a brane do not reduce the supersymmetry of the massless modes. As an example, let us consider the  $w_1p_2$  model that contains  $D_9$  and  $D5_1$  branes. After performing a T-duality along the first and the third tori, the  $D9$  branes turn into  $D5_2$  branes and the  $D5_1$  branes turn into  $D5_3$  branes, while the resulting model has momentum shifts in the first two directions. These are both orthogonal to the  $D5_3$  branes, and the corresponding massless modes have indeed  $N = 4$  supersymmetry. On the other hand, one of these shifts is parallel to the  $D5_2$  branes and breaks the corresponding supersymmetry to  $N = 2$ . Models with three shifts are more subtle, due to the  $Z_2 \times Z_2$  group structure of the transformations, but may be understood

along similar lines.

With this proviso, we can conclude this Section by giving another simple rule, that will be justified in the next Section, to predict the amount of supersymmetry for the massless modes of a brane:

*Supersymmetry is enhanced for the massless modes on a brane when the Scherk-Schwarz breaking is induced by momentum shifts orthogonal to it, or in all cases that may be linked to this by suitable T-dualities.*

#### 4. Structure of the shift orientifolds

In this Section we would like to describe how to construct the vacuum amplitudes for the open descendants of  $Z_2 \times Z_2$  shift-orbifold models.

In all cases the starting point is a deformation of the torus amplitude (2.1), where momentum or winding shifts induce corresponding modifications of the twisted contributions. For instance, for the case of two momentum shifts the torus amplitude is

$$\begin{aligned} \mathcal{T} = & \frac{1}{4} \left\{ |T_{oo}|^2 \Lambda_1 \Lambda_2 \Lambda_3 + |T_{og}|^2 \Lambda_1 \left| \frac{4\eta^2}{\theta_2^2} \right|^2 + |T_{of}|^2 (-1)^{m_2} \Lambda_2 \left| \frac{4\eta^2}{\theta_2^2} \right|^2 + |T_{oh}|^2 (-1)^{m_3} \Lambda_3 \left| \frac{4\eta^2}{\theta_2^2} \right|^2 \right. \\ & + |T_{go}|^2 \Lambda_1 \left| \frac{4\eta^2}{\theta_4^2} \right|^2 + |T_{gg}|^2 \Lambda_1 \left| \frac{4\eta^2}{\theta_3^2} \right|^2 + |T_{fo}|^2 \Lambda_2^{n_2+1/2} \left| \frac{4\eta^2}{\theta_4^2} \right|^2 \\ & \left. + |T_{ff}|^2 (-1)^{m_2} \Lambda_2^{n_2+1/2} \left| \frac{4\eta^2}{\theta_3^2} \right|^2 + |T_{ho}|^2 \Lambda_3^{n_3+1/2} \left| \frac{4\eta^2}{\theta_4^2} \right|^2 + |T_{hh}|^2 (-1)^{m_3} \Lambda_3^{n_3+1/2} \left| \frac{4\eta^2}{\theta_3^2} \right|^2 \right\}. \end{aligned} \quad (4.1)$$

In all these deformed models, the independent orbit related to the discrete torsion is absent.

The corresponding open descendants are essentially determined by the direct-channel Klein-bottle amplitude  $\mathcal{K}$  and by the transverse-channel annulus amplitude  $\tilde{\mathcal{A}}$ . Moreover, the former, to which we now turn, is fully specified by the corresponding table ( $\sigma_1$  or  $\sigma_2$ ) and by our choice of working with a conventional  $\Omega$  projection.

The Klein-bottle amplitudes are generically affected by the shifts, that can make the

transverse-channel contributions massive. As in the supersymmetric case discussed in Section 2, the direct-channel amplitude,  $\mathcal{K}$ , includes four distinct contributions, corresponding to  $P_1P_2P_3$ ,  $P_1W_2W_3$ ,  $W_1P_2W_3$  and  $W_1W_2P_3$  where, as in previous Sections,  $P_i$  and  $W_i$  indicate lattice sums restricted to zero windings or zero momenta, respectively. These four terms reflect the  $Z_2 \times Z_2$  structure of these models, and determine their content of  $D9$ ,  $D5_1$ ,  $D5_2$  and  $D5_3$  branes. Whenever these terms are accompanied in  $\mathcal{K}$  by phases induced by the shifts, the corresponding vacuum-channel contributions are lifted in mass, and tadpole conditions eliminate the corresponding branes. In order to describe this effect in some detail, let us identify the two types of projected lattice operators corresponding to the shift matrices  $\sigma_1$  and  $\sigma_2$  of eq. (3.1) :

$$V_1 = e^{i(p_{1L}x_{1L} + p_{2L}x_{2L} + p_{3L}x_{3L} + (L \leftrightarrow R))} + (-1)^{\delta_1 + \delta_2} e^{i(p_{1L}x_{1L} - p_{2L}x_{2L} - p_{3L}x_{3L} + (L \leftrightarrow R))} \\ + (-1)^{\delta_2 + \delta_3} e^{i(-p_{1L}x_{1L} + p_{2L}x_{2L} - p_{3L}x_{3L} + (L \leftrightarrow R))} + (-1)^{\delta_1 + \delta_3} e^{i(-p_{1L}x_{1L} - p_{2L}x_{2L} + p_{3L}x_{3L} + (L \leftrightarrow R))}, \quad (4.2)$$

$$V_2 = e^{i(p_{1L}x_{1L} + p_{2L}x_{2L} + p_{3L}x_{3L} + (L \leftrightarrow R))} + (-1)^{\delta_1} e^{i(p_{1L}x_{1L} - p_{2L}x_{2L} - p_{3L}x_{3L} + (L \leftrightarrow R))} \\ + (-1)^{\delta_2 + \delta_3} e^{i(-p_{1L}x_{1L} + p_{2L}x_{2L} - p_{3L}x_{3L} + (L \leftrightarrow R))} + (-1)^{\delta_1 + \delta_2 + \delta_3} e^{i(-p_{1L}x_{1L} - p_{2L}x_{2L} + p_{3L}x_{3L} + (L \leftrightarrow R))}, \quad (4.3)$$

where  $(-1)^\delta$  is  $(-1)^m$  for a momentum shift and  $(-1)^n$  for a winding shift. These operators combine with diagonal untwisted oscillator contributions, such as  $|\tau_{oo}|^2$ , and can thus flow both in the Klein bottle  $\mathcal{K}$  and in the transverse-channel annulus amplitude  $\tilde{\mathcal{A}}$ . As we have seen, the four types of contributions to  $\mathcal{K}$ , that correspond to  $P_1P_2P_3$ ,  $P_1W_2W_3$ ,  $W_1P_2W_3$  and  $W_1W_2P_3$ , involve restricted lattice sums. They arise from operators like those in eqs. (4.2) and (4.3), specialized to the cases of vanishing momenta or windings, that are therefore eigenvectors of  $\Omega$ . Moreover, for the  $P_1P_2P_3$  case the eigenvalue is always one, while in the other cases it is simple to see from eq. (4.2) that the eigenvalues are  $(-1)^{\delta_1 + \delta_2}$ ,  $(-1)^{\delta_2 + \delta_3}$  and  $(-1)^{\delta_2 + \delta_3}$  for the  $\sigma_1$  case, and  $(-1)^{\delta_1}$ ,  $(-1)^{\delta_2 + \delta_3}$  and  $(-1)^{\delta_1 + \delta_2 + \delta_3}$  for the  $\sigma_2$  case. The end result is that, aside from twisted contributions, the Klein bottle projections for the two

cases may be written in the form

$$\mathcal{K}_1 = \frac{1}{8} \left\{ P_1 P_2 P_3 + (-1)^{\delta_1 + \delta_2} P_1 W_2 W_3 + (-1)^{\delta_2 + \delta_3} W_1 P_2 W_3 + (-1)^{\delta_1 + \delta_3} W_1 W_2 P_3 \right\} T_{oo} \quad , \quad (4.4)$$

and

$$\mathcal{K}_2 = \frac{1}{8} \left\{ P_1 P_2 P_3 + (-1)^{\delta_1} P_1 W_2 W_3 + (-1)^{\delta_2 + \delta_3} W_1 P_2 W_3 + (-1)^{\delta_1 + \delta_2 + \delta_3} W_1 W_2 P_3 \right\} T_{oo} \quad . \quad (4.5)$$

In order to describe the brane content of a given model, one can then specialize these equations to the corresponding choice of (momentum or winding) shifts. Whenever a phase has a nontrivial effect on a restricted lattice sum, the corresponding transverse-channel contribution is lifted in mass, and the tadpole conditions eliminate the corresponding brane. For instance, for the  $P_1 W_2 W_3$  sum this is the case for a momentum shift along the first torus, and/or for winding shifts along the other two tori. In order to discuss a concrete example, let us consider the  $p_{23}$  model. In this case the only phases present are  $\delta_2 = m_2$  and  $\delta_3 = m_3$ , while the corresponding multiplication table is  $\sigma_2$ . Then, aside from twisted contributions

$$\mathcal{K} = \frac{1}{8} \left\{ P_1 P_2 P_3 + P_1 W_2 W_3 + (-1)^{m_2} W_1 P_2 W_3 + (-1)^{m_3} W_1 W_2 P_3 \right\} T_{oo} \quad , \quad (4.6)$$

and consequently one is left only with  $D9$  and  $D5_1$  branes.

The twisted contributions to the Klein-bottle amplitude can then be induced most conveniently, in all models, from the terms in  $\tilde{\mathcal{K}}$  at the origin of the lattices, that they are to complete into perfect squares. We shall see several examples of this procedure in the following Sections.

The other crucial ingredient of the construction, to which we now turn, is the transverse-channel annulus amplitude  $\tilde{\mathcal{A}}$ . This presents some subtleties, since the shift orbifold restricts the allowed untwisted modes. These constraints have a simple geometrical origin: in general, the fixed tori of one operation are paired by the others and form multiplets, whose

members must accommodate identical brane sets. As a result, branes are accompanied by a number of images, and the restrictions on the form of  $\tilde{\mathcal{A}}$  determine their minimal configurations. This is reminiscent of what happens in ordinary orbifolds when, by a continuous deformation, a brane is moved off a fixed point, but in shift orbifolds the presence of image branes is in general unavoidable.

In order to prepare the grounds for the discussion of the shift orbifolds, it is instructive to see how the displacement of branes works in the  $T^4/Z_2$  orbifold. This phenomenon, first discussed in [21], may be given a complete description in conformal field theory starting from the torus amplitude

$$\mathcal{T} = \frac{1}{2} \left\{ \Lambda^4 |Q_o + Q_v|^2 + |Q_o - Q_v|^2 \left| \frac{2\eta}{\theta_2} \right|^4 + |Q_s + Q_c|^2 \left| \frac{2\eta}{\theta_4} \right|^4 + |Q_s - Q_c|^2 \left| \frac{2\eta}{\theta_3} \right|^4 \right\} , \quad (4.7)$$

where  $\Lambda$  denotes a one-dimensional toroidal lattice sum and, as usual, we have introduced the four supersymmetric combinations of  $SO(4)$  characters

$$\begin{aligned} Q_o &= V_4 O_4 - C_4 C_4 , & Q_v &= O_4 V_4 - S_4 S_4 , \\ Q_s &= O_4 C_4 - S_4 O_4 , & Q_c &= V_4 S_4 - C_4 V_4 . \end{aligned} \quad (4.8)$$

The Klein-bottle amplitudes are then

$$\begin{aligned} \mathcal{K} &= \frac{1}{4} \left\{ (Q_o + Q_v)(P^4 + W^4) + 2 \times 16(Q_s + Q_c) \left( \frac{\eta}{\theta_4} \right)^2 \right\} , \\ \tilde{\mathcal{K}} &= \frac{2^5}{4} \left\{ (Q_o + Q_v)(v(W^e)^4 + \frac{1}{v}(P^e)^4) + 2(Q_o - Q_v) \left( \frac{2\eta}{\theta_2} \right)^2 \right\} , \end{aligned} \quad (4.9)$$

where  $P^4$  and  $W^4$  denote the restrictions of the lattice sum  $\Lambda^4$  to zero windings and to zero momenta, respectively.

The simplest configuration, where all  $D5$  branes are at the same fixed point and no Wilson lines are introduced, results in the gauge group  $U(16)_9 \times U(16)_5$ . The familiar spectrum [20, 21] comprises two pairs of hypermultiplets in the  $(120, 1)$  and  $(1, 120)$  from the 99 and 55 sectors, and an additional 59 hypermultiplet in the  $(16, 16)$ .

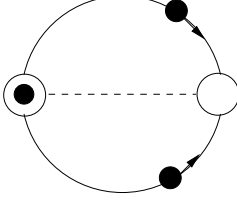


Figure 1. Pairs of image branes moved away from a fixed point.

If some pairs of  $D5$  branes are moved a distance  $2\pi\alpha R$  away from the fixed point along the last circle, the other transverse-channel amplitudes become

$$\begin{aligned}
 \tilde{\mathcal{A}} &= \frac{2^{-5}}{4} \left\{ (Q_o + Q_v) \left[ N^2 v W^4 + \frac{1}{v} \sum_m (D + \frac{\delta}{2} e^{2i\pi\alpha m} + \frac{\delta}{2} e^{-2i\pi\alpha m})^2 P^3 P_m \right] \right. \\
 &\quad \left. + 2N(D+\delta)(Q_o - Q_v) \left( \frac{2\eta}{\theta_2} \right)^2 + 4(Q_s + Q_c) (R_N^2 + R_D^2) \left( \frac{2\eta}{\theta_4} \right)^2 - 2R_N R_D (Q_s - Q_c) \left( \frac{2\eta}{\theta_3} \right)^2 \right\}, \\
 \tilde{\mathcal{M}} &= -\frac{1}{2} \left\{ (\hat{Q}_o + \hat{Q}_v) \left[ N v (W^e)^4 + \frac{1}{v} \sum_m (D + \frac{\delta}{2} e^{4i\pi\alpha m} + \frac{\delta}{2} e^{-4i\pi\alpha m}) (P^e)^3 P_{2m} \right] \right. \\
 &\quad \left. + (N + D + \delta)(\hat{Q}_o - \hat{Q}_v) \left( \frac{\hat{\eta}}{\hat{\theta}_2} \right)^2 \right\}, \tag{4.10}
 \end{aligned}$$

and thus the corresponding direct-channel amplitudes are

$$\begin{aligned}
 \mathcal{A} &= \frac{1}{4} \left\{ (Q_o + Q_v) \left[ N^2 P^4 + (D^2 + \frac{\delta^2}{2}) W^4 + \frac{\delta^2}{4} W^3 (W_{2\alpha} + W_{-2\alpha}) + D\delta W^3 (W_\alpha + W_{-\alpha}) \right] \right. \\
 &\quad \left. + 2N(D + \delta)(Q_s + Q_c) \left( \frac{\eta}{\theta_4} \right)^2 + (Q_o - Q_v) (R_N^2 + R_D^2) \left( \frac{2\eta}{\theta_2} \right)^2 + 2R_N R_D (Q_s - Q_c) \left( \frac{\eta}{\theta_3} \right)^2 \right\}, \\
 \mathcal{M} &= -\frac{1}{4} \left\{ (\hat{Q}_o + \hat{Q}_v) \left[ N P^4 + D W^4 + \frac{\delta}{2} W^3 (W_{2\alpha} + W_{-2\alpha}) \right] \right. \\
 &\quad \left. - (\hat{Q}_o - \hat{Q}_v) (N + D + \delta) \left( \frac{2\hat{\eta}}{\hat{\theta}_2} \right)^2 \right\}. \tag{4.11}
 \end{aligned}$$

Here  $N$  denotes the total number of  $D9$  branes,  $D$  denotes the total number of  $D5$  branes left at the origin,  $\delta$  counts the number of displaced branes, and  $R_N$  and  $R_D$  account for the effect of the orbifold breaking on the Chan-Paton charges at the fixed points. If  $\alpha \neq 1/2$ , the moved branes are also away from the other fixed point on the circle, and the corresponding breaking terms  $R_\delta$  are absent. Since the consistency of the conformal

theory in both channels allows only breaking terms for branes sitting at fixed points, one is forced to let  $\delta = 2d$ , thus effectively splitting the charge between image branes. This is somewhat reminiscent of the splitting induced by a quantized NS  $B_{ab}$  [11], and indeed the rank of the gauge group is correspondingly reduced. These features reflect the geometry of the brane configuration, that includes pairs of images interchanged by orbifold operations. The structure of  $\mathcal{M}$  implies that in this case the gauge groups carried by the displaced branes are symplectic and have a reduced rank [21]. We would like to stress that, while in the absence of breaking terms the  $\delta$  contributions appear to have enhanced supersymmetry, this is actually reduced by the Möbius projection, as was the case for the supersymmetric  $Z_2 \times Z_2$  model without discrete torsion discussed in Section 2. On the other hand, in the following Sections we shall see that in shift orbifolds  $\mathcal{M}$  respects the enhancement of supersymmetry. Summarizing, for  $\alpha \neq 1/2$  the  $D5$  gauge group generically breaks from  $U(16)$  to  $U(16 - 2d) \times USp(2d)$ . On the other hand, for  $\alpha = 1/2$  the pairs of images meet at the other fixed point on the circle. The orbifold breakings are now allowed for all  $D5$  branes, and the rank of the  $D5$  gauge group is correspondingly enhanced. In the transverse channel, the modified breaking terms

$$\frac{2^{-5}}{4} \left\{ 16(Q_s + Q_c) (R_N^2 + R_D^2 + R_\delta^2) \left(\frac{\eta}{\theta_4}\right)^2 - 8R_N(R_D + R_\delta) (Q_s - Q_c) \left(\frac{\eta}{\theta_3}\right)^2 \right\} \quad (4.12)$$

reflect the position of the  $D5$  branes, that now occupy both fixed points along the circle, and indeed at the origin eq. (4.12) becomes

$$\frac{1}{4} \left[ (R_N - 4R_D)^2 + (R_N - 4R_\delta)^2 + 14R_N^2 \right] \quad . \quad (4.13)$$

These results have a direct bearing on the main subject of this paper. Indeed, if some orbifold operation were to interchange the two fixed points where we have placed the  $D5$  branes, as will be the case in the  $Z_2 \times Z_2$  shift orientifolds discussed in the following Sections, one would be forced to set  $D = \delta$  and  $R_D = R_\delta$ , and as a result for  $\alpha = 1/2$   $\tilde{\mathcal{A}}$  would include the projector

$$\Pi = \frac{1}{2} (1 + (-1)^m) \quad . \quad (4.14)$$

Summarizing, the presence of brane multiplets in the vacuum configuration reflects itself in the presence of corresponding projection operators in  $\tilde{\mathcal{A}}$ .

We can now turn to describe how the projection operators may be determined for the two classes of models corresponding to  $\sigma_1$  and  $\sigma_2$ . The starting point are the projected lattice operators  $V_1$  and  $V_2$  of eqs. (4.2) and (4.3), that combine in the closed spectrum with diagonal untwisted oscillator contributions, such as  $\tau_{oo}$ . They are clearly allowed in  $\tilde{\mathcal{A}}$ , and determine the  $NN$  and  $D_i D_i$  terms, and thus the brane content of the models. If we let the corresponding states flow in the tube, all terms in  $V_1$  and  $V_2$ , being degenerate in mass, are accompanied by the same power of  $q$ , and thus one inherits the projectors

$$\Pi_1 \sim 1 + (-1)^{\delta_1 + \delta_2} + (-1)^{\delta_2 + \delta_3} + (-1)^{\delta_1 + \delta_3} , \quad (4.15)$$

$$\Pi_2 \sim 1 + (-1)^{\delta_1} + (-1)^{\delta_2 + \delta_3} + (-1)^{\delta_1 + \delta_2 + \delta_3} . \quad (4.16)$$

In order to give a concrete example, let us refer again to the  $p_{23}$  model, that as we have seen has  $D9$  and  $D5_1$  branes. In this case

$$\Pi = \frac{1}{2} \left( 1 + (-1)^{m_2 + m_3} \right) , \quad (4.17)$$

and all states flowing in the transverse channel of the annulus must have correlated momenta, both even or both odd in the corresponding two circles of the last two tori. Clearly,  $\Pi$  has no effect on the  $D9$  contribution, that in the transverse-channel annulus amplitude only involves windings. However, it does play a crucial role for the sector associated to the  $D5_1$  brane. In this case, the transverse-channel contribution corresponds to  $W_1 P_2 P_3$ , and the projection affects the momenta in the last two sums. Since the Poisson transform of the restricted sum is proportional to  $P_1 (W_2 W_3 + W_2^{n+1/2} W_3^{n+1/2})$ , where the  $W_i^{n+1/2}$  in the last two factors denote shifted sums, in the direct channel  $\Pi$  gives rise to a doublet of branes. As we have seen, this is precisely the type of configuration required by the structure of the shift orbifold.

## 5. An interesting example with $N = 2 \rightarrow N = 1$ breaking

In this Section we would like to describe in some detail an interesting class of models, obtained introducing in the table  $\sigma_2$  of eq. (3.1) momentum shifts  $p_2$  and  $p_3$  in two lattice directions, where  $N = 2$  supersymmetry is spontaneously broken to  $N = 1$ . The previous analysis reveals that, in addition to  $D9$ -branes, they also contain  $D5_1$  branes. They have the rather interesting feature of displaying various numbers of supersymmetries in the bulk and on the branes in a relatively simple setting. The thumb rule of Section 3 predicts in this case  $N = 1$  supersymmetry for the  $D9$  branes, since the two shifts are parallel to their world volume, and  $N = 2$  supersymmetry for the massless modes of the  $D5_1$  branes, since they are acted upon by the  $g$  projection, while the two shifts are orthogonal to their world volume.

The direct and transverse Klein bottle amplitudes for this model

$$\begin{aligned} \mathcal{K} &= \frac{1}{8} \left\{ T_{oo} [P_1 P_2 P_3 + P_1 W_2 W_3 + W_1 (-1)^{m_2} P_2 W_3 + W_1 W_2 (-1)^{m_3} P_3] + 2 \times 16 T_{go} P_1 \left( \frac{\eta}{\theta_4} \right)^2 \right\}, \\ \tilde{\mathcal{K}} &= \frac{2^5}{8} \left\{ T_{oo} [v_1 v_2 v_3 W_1^e W_2^e W_3^e + \frac{v_1}{v_2 v_3} W_1^e P_2^e P_3^e + \frac{v_2}{v_1 v_3} P_1^e W_2^o P_3^e + \frac{v_3}{v_1 v_2} P_1^e P_2^e W_3^o] \right. \\ &\quad \left. + 2 T_{og} v_1 W_1^e \left( \frac{2\eta}{\theta_2} \right)^2 \right\} \quad , \end{aligned} \quad (5.1)$$

are determined by the rules described in Section 3. In particular, the twisted contribution is fixed by the behavior of  $\tilde{\mathcal{K}}$  at the origin of the lattices, and ensures that the various independent sectors of the spectrum have reflection coefficients that are perfect squares. Indeed:

$$\tilde{\mathcal{K}}_0 = \frac{2^5}{8} \left\{ (\tau_{oo} + \tau_{og}) \left( \sqrt{v_1 v_2 v_3} + \sqrt{\frac{v_1}{v_2 v_3}} \right)^2 + (\tau_{of} + \tau_{oh}) \left( \sqrt{v_1 v_2 v_3} - \sqrt{\frac{v_1}{v_2 v_3}} \right)^2 \right\}. \quad (5.2)$$

The vacuum channel annulus amplitude

$$\tilde{\mathcal{A}} = \frac{2^{-5}}{8} \left\{ T_{oo} \left[ N^2 v_1 v_2 v_3 W_1 W_2 W_3 + D_1^2 \frac{v_1}{v_2 v_3} W_1 (P_2^e P_3^e + P_2^o P_3^o) \right] \right\}$$

$$\begin{aligned}
 & + 4(G^2 + 2G_1^2)T_{go}W_1v_1\left(\frac{2\eta}{\theta_4}\right)^2 + 4F^2T_{fo}W_2^{n+1/2}v_2\left(\frac{2\eta}{\theta_4}\right)^2 + 4H^2T_{ho}W_3^{n+1/2}v_3\left(\frac{2\eta}{\theta_4}\right)^2 \\
 & + 2ND_1T_{og}W_1v_1\left(\frac{2\eta}{\theta_2}\right)^2 + 4GG_1T_{gg}W_1v_1\left(\frac{2\eta}{\theta_3}\right)^2 \}
 \end{aligned} \tag{5.3}$$

inherits the projection operator

$$\Pi = \frac{1}{2} [1 + (-1)^{m_2+m_3}] \tag{5.4}$$

that, as we have seen in the previous Section, restricts the 55 contribution to the even-even (*ee*) and odd-odd (*oo*) subsets of momentum eigenvalues in the last two tori.

Leaving a discussion of the breaking terms momentarily aside, by an *S* transformation we can turn this expression into the direct-channel annulus amplitude

$$\begin{aligned}
 \mathcal{A} = & \frac{1}{8} \left\{ T_{oo} \left[ N^2 P_1 P_2 P_3 + \frac{D_1^2}{2} P_1 (W_2 W_3 + W_2^{n+1/2} W_3^{n+1/2}) \right] + (G^2 + 2G_1^2) T_{og} P_1 \left(\frac{2\eta}{\theta_2}\right)^2 \right. \\
 & + F^2 T_{of} (-1)^{m_2} P_2 \left(\frac{2\eta}{\theta_2}\right)^2 + H^2 T_{oh} (-1)^{m_3} P_3 \left(\frac{2\eta}{\theta_2}\right)^2 + 2ND_1 T_{go} P_1 \left(\frac{\eta}{\theta_4}\right)^2 \\
 & \left. + 4GG_1 T_{gg} P_1 \left(\frac{\eta}{\theta_3}\right)^2 \right\} .
 \end{aligned} \tag{5.5}$$

Whereas the 99 strings are rather conventional, and have the usual three projection terms, although affected by the momentum shifts as in the simpler models of [6, 7], the configuration of the 55 strings is more peculiar, and admits a nice geometrical interpretation: it corresponds to a doublet of branes, associated to a pair of tori fixed by *g* and interchanged by *f* and *h*. Only the *g* projection is present, since in this sector the physical states are combinations of pairs localized on the image branes. In this case the *full D5*<sub>1</sub> spectrum, not only its massless modes, has enhanced supersymmetry. We have already stressed that multiplets of branes are a generic feature of these shift orbifolds. Even if one attempts to insert all branes at a fixed point, the other operations typically move them, and give rise to multiple images. This is summarized for this class of models in figure 2, where the three axes refer to the three two-tori  $T_{45}$ ,  $T_{67}$  and  $T_{89}$ . As usual, the massive untwisted excitations of these orbifold models have enhanced supersymmetry, although they have only a fraction

of the lattice modes present in the toroidal case. More precisely, the  $g$  projection forbids this extension in the first torus, while in the second and third tori the projected combinations of lattice states have indeed  $N = 2$  supersymmetry in the 99 sector and  $N = 4$  supersymmetry in the 55 sector.

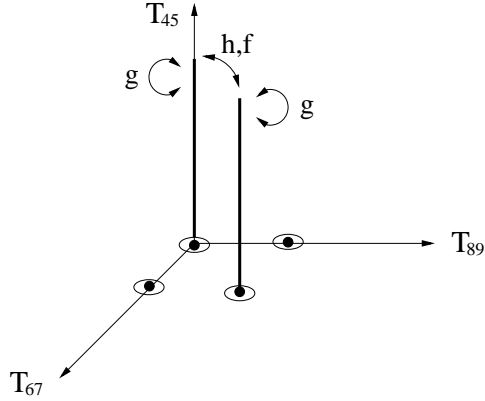


Figure 2.  $D5_1$  brane configuration for the  $p_{23}$  model

The previous considerations determine the structure of the breaking terms in the transverse channel: as we have anticipated, the  $D5_1$  branes occupy a pair of fixed tori, while all others are empty. Then, according to the rule discussed in the previous Section, in the transverse channel the breaking terms are to group into the structures

$$\frac{2}{4}(G \mp 4G_1)^2 + \frac{14}{4}G^2 , \quad (5.6)$$

precisely as demanded by the direct-channel amplitude  $\mathcal{A}$ . The relative factor between  $G$  and  $G_1$  in the first term counts the number of occupied fixed points; more precisely in all these models it is equal to

$$\sqrt{\frac{\# \text{ of fixed points}}{\# \text{ of occupied fixed points}}} . \quad (5.7)$$

At the origin of the lattices, the untwisted contribution to the transverse-channel annulus amplitude is

$$\tilde{\mathcal{A}}_0 = \frac{2^{-5}}{8} \left\{ (\tau_{oo} + \tau_{og}) \left( N \sqrt{v_1 v_2 v_3} + D_1 \sqrt{\frac{v_1}{v_2 v_3}} \right)^2 + (\tau_{of} + \tau_{oh}) \left( N \sqrt{v_1 v_2 v_3} - D_1 \sqrt{\frac{v_1}{v_2 v_3}} \right)^2 \right\} , \quad (5.8)$$

and, together with  $\tilde{\mathcal{K}}_0$  of eq. (5.2), determines the transverse-channel Möbius amplitude

$$\begin{aligned}\tilde{\mathcal{M}} = & -\frac{1}{4}\left\{\hat{T}_{oo}\left[Nv_1v_2v_3W_1^eW_2^eW_3^e+D_1\frac{v_1}{v_2v_3}W_1^eP_2^eP_3^e\right]+\hat{T}_{og}(N+D_1)W_1^ev_1\left(\frac{2\hat{\eta}}{\hat{\theta}_2}\right)^2\right. \\ & \left.+N\hat{T}_{of}W_2^ov_2\left(\frac{2\hat{\eta}}{\hat{\theta}_2}\right)^2-N\hat{T}_{oh}W_3^ov_3\left(\frac{2\hat{\eta}}{\hat{\theta}_2}\right)^2\right\} .\end{aligned}\quad (5.9)$$

Finally, a  $P$  transformation determines the direct-channel Möbius projection

$$\begin{aligned}\mathcal{M} = & -\frac{1}{8}\left\{\hat{T}_{oo}\left[NP_1P_2P_3+D_1P_1W_2W_3\right]-\hat{T}_{og}(D_1+N)P_1\left(\frac{2\hat{\eta}}{\hat{\theta}_2}\right)^2-N\hat{T}_{of}(-1)^{m_2}P_2\left(\frac{2\hat{\eta}}{\hat{\theta}_2}\right)^2\right. \\ & \left.+N\hat{T}_{oh}(-1)^{m_3}P_3\left(\frac{2\hat{\eta}}{\hat{\theta}_2}\right)^2\right\} ,\end{aligned}\quad (5.10)$$

whose contributions at the origin of the lattices imply that both types of gauge groups are unitary. The untwisted tadpole conditions

$$N = D_1 = 32 \quad (5.11)$$

fix the (maximal) size of the two gauge groups, while the twisted tadpole conditions

$$G = G_1 = 0 \quad (5.12)$$

are identically satisfied if one parametrizes the charges according to

$$\begin{aligned}N &= o + g + \bar{o} + \bar{g} , & G &= i(o + g - \bar{o} - \bar{g}) , \\ H &= (o - g + \bar{o} - \bar{g}) , & F &= i(o - g - \bar{o} + \bar{g}) , \\ D_1 &= 2(d + \bar{d}) , & G_1 &= i(d - \bar{d}) ,\end{aligned}\quad (5.13)$$

provided  $o + g = 16$  and  $d = 8$ . The massless modes from the open sector are then summarized in

$$\begin{aligned}\mathcal{A}_0 + \mathcal{M}_0 = & (o\bar{o} + g\bar{g})\tau_{oo} + (o\bar{g} + g\bar{o})\tau_{og} + (og + \bar{o}\bar{g})\tau_{of} \\ & + \left[\frac{o(o-1)}{2} + \frac{g(g-1)}{2} + \frac{\bar{o}(\bar{o}-1)}{2} + \frac{\bar{g}(\bar{g}-1)}{2}\right]\tau_{oh} \\ & + d\bar{d}(\tau_{oo} + \tau_{og}) + \left[\frac{d(d-1)}{2} + \frac{\bar{d}(\bar{d}-1)}{2}\right](\tau_{of} + \tau_{oh}) \\ & + [(o+g)d + (\bar{o}+\bar{g})\bar{d}](\tau_{gf} + \tau_{gh}) ,\end{aligned}\quad (5.14)$$

while the gauge groups allowed by the tadpole conditions in this class of models are

$$[U(o) \times U(g)]_9 \times U(8)_{5_1} . \quad (5.15)$$

The tree-level spectrum of the  $D9$  branes has  $N = 1$  supersymmetry, while the whole spectrum of the  $D5_1$  branes, orthogonal to the directions used to induce supersymmetry breaking, has indeed  $N = 2$  supersymmetry. This is one more instance of the phenomenon discussed in [6, 7], and extended to the whole spectrum in [10], as suggested in [8]. The massless spectrum is not chiral, and includes 99 chiral multiplets in the representations  $(o(o-1)/2, 1, 1)$ ,  $(1, g(g-1)/2, 1)$ ,  $(o, \bar{g}, 1)$ ,  $(o, g, 1)$  and their hermitian conjugates, one pair of 55 hypermultiplets in the representation  $(1, 1, d(d-1)/2)$ , and 59 hypermultiplets in the representations  $(o, 1, d)$  and  $(1, g, d)$ .

It is instructive to discuss the behavior of this spectrum in the decompactification limit for the directions used to break supersymmetry. In [7] we studied some simpler examples, where momentum (or winding) shifts along one coordinate were combined with a single  $Z_2$  orbifold inversion in other directions. In these cases it is relatively simple to understand how, in the singular  $R \rightarrow \infty$  ( $R \rightarrow 0$ ) limit, the deformed spectrum collapses into a continuum of momentum (winding) modes with  $N=4$  supersymmetry. On the other hand, in the decompactification limit, the  $p_2p_3$  models discussed in this section recover only  $N=2$  supersymmetry. This is already a subtler setting, even in the supersymmetric case without shifts: in this limit the untwisted bulk states are still in the presence of walls, so that their momentum modes are still projected, while some twisted states are moved to infinity, together with the corresponding fixed points. In these shifted non-compact orbifolds, the momentum modes for the untwisted states merge in the limit in an extended continuum, but some of the fixed points, with the corresponding brane content, move away to infinity. Moreover, in these open-string models the singular limit is usually accompanied by the emergence of new tadpoles [14, 6], that may be eliminated arranging for *local* cancellations [26]. Actually, in this case if only one of the radii  $R_2$  and  $R_3$  tends to infinity, the local

tadpole conditions are identically satisfied. This fact has a simple geometric reason: the image doublets of  $D5_1$  branes saturate locally the RR charge. We would like to stress that the identified images carry the same gauge group, a fact to be contrasted with the simpler toroidal setting of [14]. On the other hand, when both radii are large, the saturation requires a further breaking of the  $D5_1$  gauge group to  $U(4) \times U(4)$ . In the decompactification limit of these  $p_2p_3$  models, a single set of  $D5$  branes is left, with a  $U(4)$  gauge group, while the others are moved to infinity. This limiting configuration may still be linked to the conventional  $U(16)_9 \times U(16)_5$  setting of the compact  $T^4/Z_2$  orbifold, albeit in a  $(U(4)_5)^4$  configuration, and where 12 of the  $D5_1$  branes have been moved to infinity in the decompactification limit.

## 6. Freely-acting orbifold models with two $D5$ branes

In this Section we describe other classes of shift models of this type, with two  $D5$  branes. Our aim is to give a geometrical interpretation of the corresponding brane multiplets and to exhibit their  $M$  theory limits, whenever they exist, as well as their massless spectra. For the sake of brevity, we shall only display direct-channel amplitudes.

### 6.1. One momentum shift

This case corresponds to introducing a single momentum shift  $p_3$  in the table  $\sigma_1$  of eq. (3.1). The resulting models contain  $D9$ ,  $D5_1$  and  $D5_2$  branes. The direct-channel Klein bottle amplitude is

$$\begin{aligned} \mathcal{K} = & \frac{1}{8} \left\{ T_{oo} \left[ P_1 P_2 P_3 + P_1 W_2 W_3 + W_1 P_2 W_3 + W_1 W_2 (-1)^{m_3} P_3 \right] \right. \\ & \left. + 2 \times 16 T_{go} P_1 \left( \frac{\eta}{\theta_4} \right)^2 + 2 \times 16 T_{fo} P_2 \left( \frac{\eta}{\theta_4} \right)^2 + 2 \times 16 T_{ho} W_3^{n+1/2} \left( \frac{\eta}{\theta_4} \right)^2 \right\} , \quad (6.1) \end{aligned}$$

the direct-channel annulus amplitude is

$$\mathcal{A} = \frac{1}{8} \left\{ T_{oo} \left[ N^2 P_1 P_2 P_3 + \frac{D_1^2}{2} P_1 W_2 (W_3 + W_3^{n+1/2}) + \frac{D_2^2}{2} W_1 P_2 (W_3 + W_3^{n+1/2}) \right] \right.$$

$$\begin{aligned}
& + (G^2 + 2G_1^2)T_{og}P_1 \left( \frac{2\eta}{\theta_2} \right)^2 + (F^2 + 2F_2^2)T_{of}P_2 \left( \frac{2\eta}{\theta_2} \right)^2 + H^2 T_{oh}(-1)^{m_3} P_3 \left( \frac{2\eta}{\theta_2} \right)^2 \\
& + 2ND_1T_{go}P_1 \left( \frac{\eta}{\theta_4} \right)^2 + 2ND_2T_{fo}P_2 \left( \frac{\eta}{\theta_4} \right)^2 + D_1D_2T_{ho}(W_3^{n+1/4} + W_3^{n+3/4}) \left( \frac{\eta}{\theta_4} \right)^2 \\
& + 4GG_1T_{gg}P_1 \left( \frac{\eta}{\theta_3} \right)^2 + 4FF_2T_{ff}P_2 \left( \frac{\eta}{\theta_3} \right)^2 \} , \tag{6.2}
\end{aligned}$$

and finally the Möbius projection is

$$\begin{aligned}
\mathcal{M} = & -\frac{1}{8} \left\{ \hat{T}_{oo} \left[ NP_1P_2P_3 + D_1P_1W_2W_3 + D_2W_1P_2W_3 \right] - \hat{T}_{og}(D_1 + N)P_1 \left( \frac{2\hat{\eta}}{\hat{\theta}_2} \right)^2 \right. \\
& \left. - \hat{T}_{of}(D_2 + N)P_2 \left( \frac{2\hat{\eta}}{\hat{\theta}_2} \right)^2 - \hat{T}_{oh}(D_2 + D_1)W_3^{n+1/2} \left( \frac{2\hat{\eta}}{\hat{\theta}_2} \right)^2 + \hat{T}_{oh}N(-1)^{m_3} P_3 \left( \frac{2\hat{\eta}}{\hat{\theta}_2} \right)^2 \right\} . \tag{6.3}
\end{aligned}$$

The corresponding brane configuration is shown in Figure 3, where the  $D5_1$  branes are parallel to the  $T_{45}$  axis and the  $D5_2$  branes are parallel to the  $T_{67}$  axis.

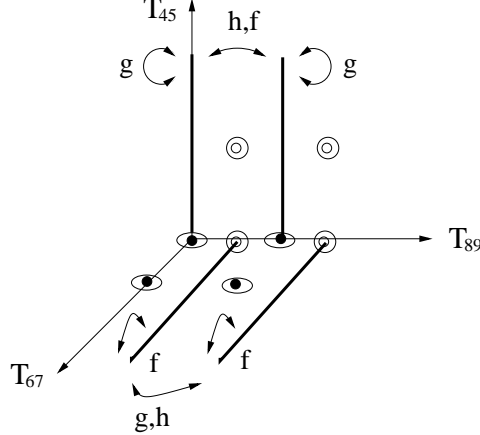


Figure 3.  $D5_1$  and  $D5_2$  brane configuration for the  $p_3$  model

We can parameterize the charges according to

$$\begin{aligned}
N &= o + g + \bar{g} + \bar{o} , & G &= i(o + g - \bar{g} - \bar{o}) , \\
H &= o - g - \bar{g} + \bar{o} , & F &= i(o - g + \bar{g} - \bar{o}) , \\
D_1 &= 2(d_1 + \bar{d}_1) , & G_1 &= i(d_1 - \bar{d}_1) , \\
D_2 &= 2(d_2 + \bar{d}_2) , & F_2 &= i(d_2 - \bar{d}_2) , \tag{6.4}
\end{aligned}$$

and the tadpole conditions

$$o + g = 16 , \quad d_1 = 8 , \quad d_2 = 8 \quad (6.5)$$

then require a gauge group

$$[U(o) \times U(g)]_9 \times [U(8)]_{5_1} \times [U(8)]_{5_2} . \quad (6.6)$$

The massless spectrum is again not chiral and has  $N = 1$  supersymmetry on the  $D9$  branes and  $N = 2$  supersymmetry on the two types of  $D5$  branes, that are orthogonal to the direction used for the breaking. The 99 spectrum contains chiral multiplets in the representations  $(o(o-1)/2, 1, 1, 1)$ ,  $(1, g(g-1)/2, 1, 1)$ ,  $(o, g, 1, 1)$  and  $(o, \bar{g}, 1, 1)$  and their conjugates. On the other hand, the 55 spectrum contains pairs of  $N = 2$  hypermultiplets in the representations  $(1, 1, d_1(d_1-1)/2, 1)$  and  $(1, 1, 1, d_2(d_2-1)/2)$ . Finally, the 59 spectrum includes hypermultiplets in the representations  $(o, 1, d_1, 1)$ ,  $(1, g, d_1, 1)$ ,  $(o, 1, 1, d_2)$  and  $(1, \bar{g}, 1, d_2)$ .

The brane content of the  $p_2p_3$  models discussed in the previous section is effectively a truncation of this, since the additional momentum shift eliminates the  $D5_2$  branes. Here one can follow more closely the decompactification limit of the single direction that accommodates the shift and, interestingly, the resulting low-lying modes originate from a superposition of states in two orbifold directions. Thus, the two orthogonal sets of  $D5$  branes are effectively *parallel* in this limit, where a more conventional  $U(16)_9 \times (U(8)_5)^2$  structure is recovered. The annulus amplitude is compatible from the start with local tadpole cancellations, because of the doublet structure of the  $D5_1$  and  $D5_2$  branes. Moreover, two sets of  $D5$  branes are present in the limit, where the corresponding  $U(8) \times U(8)$  gauge group finds the usual explanation in terms of Horava-Witten walls [22], as in the simpler examples of [6, 7].

## 6.2. One winding shift and one momentum shift

This case corresponds to introducing a winding shift  $w_2$  and a momentum shift  $p_3$  in the table  $\sigma_2$  of eq. (3.1). The resulting models contain  $D9$ ,  $D5_1$  and  $D5_2$  branes. The direct-channel Klein bottle amplitude is

$$\begin{aligned} \mathcal{K} = & \frac{1}{8} \left\{ T_{oo} \left[ P_1 P_2 P_3 + P_1 W_2 W_3 + W_1 P_2 W_3 + W_1 (-1)^{n_2} W_2 (-1)^{m_3} P_3 \right] \right. \\ & \left. + 2 \times 16 T_{go} P_1 \left( \frac{\eta}{\theta_4} \right)^2 + 2 \times 16 T_{fo} P_2^{m+1/2} \left( \frac{\eta}{\theta_4} \right)^2 + 2 \times 16 T_{ho} W_3^{n+1/2} \left( \frac{\eta}{\theta_4} \right)^2 \right\} \quad (6.7) \end{aligned}$$

the direct-channel annulus amplitude is

$$\begin{aligned} \mathcal{A} = & \frac{1}{8} \left\{ T_{oo} \left[ \frac{N^2}{2} P_1 (P_2 + P_2^{m+1/2}) P_3 + \frac{D_1^2}{2} P_1 W_2 (W_3 + W_3^{n+1/2}) \right. \right. \\ & + \frac{D_2^2}{4} W_1 (P_2 + P_2^{m+1/2}) (W_3 + W_3^{n+1/2}) \left. \right] + 2(G^2 + G_1^2) T_{og} P_1 \left( \frac{2\eta}{\theta_2} \right)^2 \\ & + 2N D_1 T_{go} P_1 \left( \frac{\eta}{\theta_4} \right)^2 + N D_2 T_{fo} (P_2^{m+1/4} + P_2^{m+3/4}) \left( \frac{\eta}{\theta_4} \right)^2 \\ & \left. \left. + D_1 D_2 T_{ho} (W_3^{n+1/4} + W_3^{n+3/4}) \left( \frac{\eta}{\theta_4} \right)^2 + 8G G_1 T_{gg} P_1 \left( \frac{\eta}{\theta_3} \right)^2 \right\} , \quad (6.8) \right. \end{aligned}$$

and finally the Möbius projection is

$$\begin{aligned} \mathcal{M} = & -\frac{1}{8} \left\{ \hat{T}_{oo} \left[ N P_1 P_2 P_3 + D_1 P_1 W_2 W_3 + D_2 W_1 P_2 W_3 \right] - \hat{T}_{og} (D_1 + N) P_1 \left( \frac{2\hat{\eta}}{\hat{\theta}_2} \right)^2 \right. \\ & \left. - \hat{T}_{of} (D_2 + N) P_2^{m+1/2} \left( \frac{2\hat{\eta}}{\hat{\theta}_2} \right)^2 - \hat{T}_{oh} (D_2 + D_1) W_3^{n+1/2} \left( \frac{2\hat{\eta}}{\hat{\theta}_2} \right)^2 \right\} . \quad (6.9) \end{aligned}$$

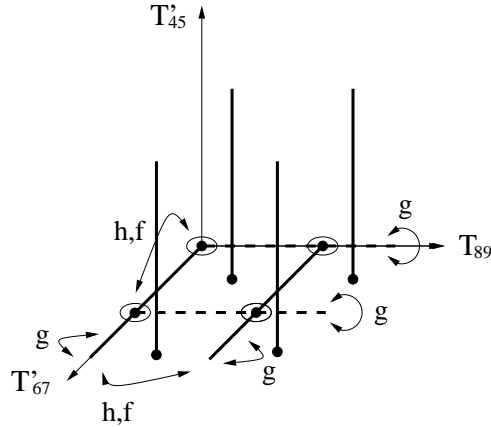


Figure 4.  $D_9$  (dashed),  $D5_1$  and  $D5_2$  branes for the  $w_2 p_3$  model.

Figure 4 shows the brane configuration, after a T-duality along  $T_{45}$  and  $T_{67}$ , that turns the  $D9$  branes into  $D5'_3$  branes (dashed), the  $D5_1$  branes into  $D5'_2$  branes (horizontal) and the  $D5_2$  branes into  $D5'_1$  branes (vertical). This model may actually be related to the  $p_2p_3$  model discussed in Section 5, via a T-duality in the first two tori. Still, we have chosen to display it, since it shows how a simple redefinition of  $\Omega$  can affect both the brane distribution and the supersymmetry of the massless modes.

We can parameterize the charges according to

$$\begin{aligned} N &= 2(n + \bar{n}) , & D_1 &= 2(d_1 + \bar{d}_1) , & D_2 &= 4d_2 , \\ G &= i(n - \bar{n}) , & G_1 &= i(d_1 - \bar{d}_1) , \end{aligned} \quad (6.10)$$

and the tadpole conditions

$$n = 8 , \quad d_1 = 8 , \quad d_2 = 8 \quad (6.11)$$

then require a gauge group

$$U(8)_9 \times U(8)_{5_1} \times SO(8)_{5_2} . \quad (6.12)$$

The massless spectrum is again not chiral and has  $N = 2$  supersymmetry on the  $D9$  and  $D5_1$  branes, and  $N = 4$  supersymmetry on the  $D5_2$  branes. Our thumb rule explains rather naturally the first two results: the  $D9$  branes are not affected by the (parallel) winding shift, while the  $D5_1$  branes are not affected by the (orthogonal) momentum shift.

Aside from the gauge multiplets, the massless spectrum contains pairs of  $N = 2$  hypermultiplets in the representation  $(28, 1, 1)$  from the  $99$  sector, in the representation  $(1, 28, 1)$  from the  $5_1 5_1$  sector, and in the representation  $(8, 8, 1)$  from the  $95_1$  sector.

In this case the interesting limits are  $R_2 \rightarrow 0$  and  $R_3 \rightarrow \infty$ . Now *all* local tadpoles are canceled, even in the simultaneous limit, without the need of any further splitting. This interesting property finds again a natural explanation in the geometry of the brane

multiplets. Indeed, while the  $D9$  and  $D5_1$  branes, orthogonal to one of the directions where shifts have been introduced, are properly arranged in doublets, the  $D5_2$  branes, orthogonal to both, are arranged in quadruplets. This structure is, again, exactly as needed to ensure local tadpole cancellation. Moreover, as quadruplets are moved by all projections, their massless modes have  $N = 4$  supersymmetry.

### 6.3. Two winding shifts and one momentum shift

This case corresponds to introducing a momentum shift  $p_3$  along the third torus, and winding shifts  $w_1$  and  $w_2$  along the others in the table  $\sigma_2$  of eq. (3.1). The resulting models contain  $D9$ ,  $D5_1$  and  $D5_2$  branes. The direct-channel Klein bottle amplitude is

$$\begin{aligned} \mathcal{K} = & \frac{1}{8} \left\{ T_{oo} \left[ P_1 P_2 P_3 + P_1 W_2 W_3 + W_1 P_2 W_3 + (-1)^{n_1} W_1 (-1)^{n_2} W_2 (-1)^{m_3} P_3 \right] \right. \\ & \left. + 2 \times 16 T_{go} P_1^{m+1/2} \left( \frac{\eta}{\theta_4} \right)^2 + 2 \times 16 T_{fo} P_2^{m+1/2} \left( \frac{\eta}{\theta_4} \right)^2 + 2 \times 16 T_{ho} W_3^{n+1/2} \left( \frac{\eta}{\theta_4} \right)^2 \right\} \quad (6.13) \end{aligned}$$

the direct-channel annulus amplitude is

$$\begin{aligned} \mathcal{A} = & \frac{1}{8} \left\{ T_{oo} \left[ \frac{N^2}{4} (P_1 + P_1^{m+1/2}) (P_2 + P_2^{m+1/2}) P_3 + \frac{D_1^2}{4} (P_1 + P_1^{m+1/2}) W_2 (W_3 + W_3^{n+1/2}) \right. \right. \\ & + \frac{D_2^2}{4} W_1 (P_2 + P_2^{m+1/2}) (W_3 + W_3^{n+1/2}) \left. \right] + T_{go} N D_1 (P_1^{m+1/4} + P_1^{m+3/4}) \left( \frac{\eta}{\theta_4} \right)^2 \\ & \left. + T_{fo} N D_2 (P_2^{m+1/4} + P_2^{m+3/4}) \left( \frac{\eta}{\theta_4} \right)^2 + T_{ho} D_1 D_2 (W_3^{n+1/4} + W_3^{n+3/4}) \left( \frac{\eta}{\theta_4} \right)^2 \right\}, \quad (6.14) \end{aligned}$$

and finally the Möbius projection is

$$\begin{aligned} \mathcal{M} = & -\frac{1}{8} \left\{ \hat{T}_{oo} \left[ N P_1 P_2 P_3 + D_1 P_1 W_2 W_3 + D_2 W_1 P_2 W_3 \right] - \hat{T}_{og} (D_1 + N) P_1^{m+1/2} \left( \frac{2\hat{\eta}}{\hat{\theta}_2} \right)^2 \right. \\ & \left. - \hat{T}_{of} (D_2 + N) P_2^{m+1/2} \left( \frac{2\hat{\eta}}{\hat{\theta}_2} \right)^2 - \hat{T}_{oh} (D_1 + D_2) W_3^{n+1/2} \left( \frac{2\hat{\eta}}{\hat{\theta}_2} \right)^2 \right\}. \quad (6.15) \end{aligned}$$

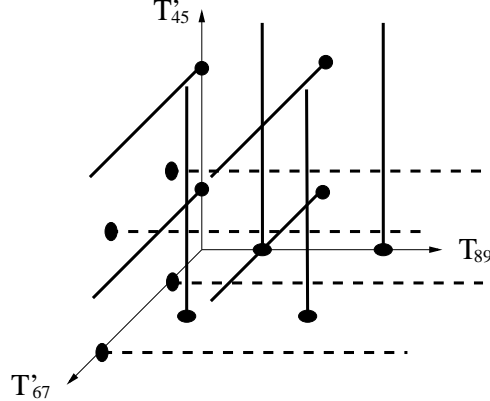


Figure 5.  $D_9$  (dashed),  $D5_1$  and  $D5_2$  branes for the  $w_1w_2p_3$  model.

Figure 5 shows the brane configuration, after a T-duality along  $T_{45}$  and  $T_{67}$ , that turns the  $D9$  branes into  $D5'_3$  branes (dashed), the  $D5_1$  branes into  $D5'_2$  branes (horizontal) and the  $D5_2$  branes into  $D5'_1$  branes (vertical).

We can parameterize the charges according to

$$N = 4n , \quad D_1 = 4d_1 , \quad D_2 = 4d_2 , \quad (6.16)$$

and the tadpole conditions

$$n = d_1 = d_2 = 8 \quad (6.17)$$

then require a gauge group

$$SO(8)_9 \times SO(8)_{5_1} \times SO(8)_{5_2} . \quad (6.18)$$

The massless spectrum is again not chiral, but now has  $N = 4$  supersymmetry on all the branes. The interesting limits are in this case  $R_1, R_2 \rightarrow 0$  and  $R_3 \rightarrow \infty$ , where the quartet structure of all types of branes guarantees again all local tadpole cancellations without the need of any further splittings.

## 7. Other models with one $D5$ brane

In this Section we provide a description of other classes of shift models with one  $D5$  brane. For the sake of brevity, we again display only direct-channel amplitudes.

### 7.1. One winding shift and one momentum shift

This case corresponds to introducing a winding shift  $w_1$  along the first torus, and a momentum shift  $p_2$  along the second torus in the table  $\sigma_2$  of eq. (3.1). The resulting models contain  $D9$  and  $D5_1$  branes. The direct-channel Klein bottle amplitude is

$$\mathcal{K} = \frac{1}{8} \left\{ T_{oo} \left[ P_1 P_2 P_3 + P_1 W_2 W_3 + W_1 (-1)^{m_2} P_2 W_3 + (-1)^{n_1} W_1 W_2 P_3 \right] + 2 \times 16 T_{go} P_1^{m+1/2} \left( \frac{\eta}{\theta_4} \right)^2 \right\}, \quad (7.1)$$

the direct-channel annulus amplitude is

$$\begin{aligned} \mathcal{A} = & \frac{1}{8} \left\{ T_{oo} \left[ \frac{N^2}{2} (P_1 + P_1^{m+1/2}) P_2 P_3 + \frac{D_1^2}{4} (P_1 + P_1^{m+1/2}) (W_2 + W_2^{n+1/2}) W_3 \right] \right. \\ & \left. + 2F^2 T_{of} (-1)^{m_2} P_2 \left( \frac{2\eta}{\theta_2} \right)^2 + T_{go} N D_1 (P_1^{m+1/4} + P_1^{m+3/4}) \left( \frac{\eta}{\theta_4} \right)^2 \right\}, \end{aligned} \quad (7.2)$$

and finally the Möbius projection is

$$\begin{aligned} \mathcal{M} = & -\frac{1}{8} \left\{ \hat{T}_{oo} \left[ N P_1 P_2 P_3 + D_1 P_1 W_2 W_3 \right] - \hat{T}_{og} (D_1 + N) P_1^{m+1/2} \left( \frac{2\hat{\eta}}{\hat{\theta}_2} \right)^2 \right. \\ & \left. - N \hat{T}_{of} (-1)^{m_2} P_2 \left( \frac{2\hat{\eta}}{\hat{\theta}_2} \right)^2 \right\}. \end{aligned} \quad (7.3)$$

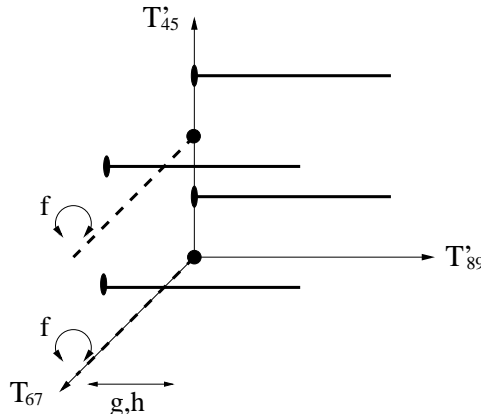


Figure 6.  $D_9$  (dashed) and  $D5_1$  branes for the  $w_1p_2$  model.

Figure 6 shows the brane configuration, after a T-duality along  $T_{45}$  and  $T_{89}$ , that turns the  $D9$  branes into  $D5'_2$  branes (dashed), the  $D5_1$  branes into  $D5'_3$  branes.

We can parameterize the charges according to

$$N = 2(n + \bar{n}) , \quad F = i(n - \bar{n}) , \quad D_1 = 4d , \quad (7.4)$$

and the tadpole conditions

$$N = D_1 = 32 , \quad (7.5)$$

then require a gauge group

$$U(8)_9 \times SO(8)_{5_1} . \quad (7.6)$$

With a discrete Wilson line on the Möbius strip, as in [20], one can also obtain a class of models with  $D9$  gauge groups  $SO(n) \times SO(16 - n)$ .

The massless spectrum is again not chiral and has  $N = 2$  supersymmetry on the  $D9$  branes and  $N = 4$  supersymmetry on the  $D5_1$  branes. Actually, the whole massive spectrum of  $D5_1$  branes has  $N = 2$  supersymmetry. Our thumb rule explains rather naturally these properties: the  $D9$  branes are not affected by the (parallel) winding shift, while the  $D5_1$  branes, orthogonal to both directions of breaking (after  $T_{45}$  duality) arrange themselves in a quartet geometry, with  $N = 4$  supersymmetry. The multiplet structure of the branes is, once more, directly compatible with all local tadpole cancellations. Aside from the gauge multiplets, the spectrum contains pairs of  $N = 2$  hypermultiplets in the representation  $(28, 1)$  from the 99 sector.

## 7.2. One winding shift and two momentum shifts

This case corresponds to introducing a winding shift  $w_1$  along the first torus, and two momentum shifts  $p_2$  and  $p_3$  along the other two tori in the table  $\sigma_2$  of eq. (3.1). The

resulting models contain  $D9$  and  $D5_1$  branes. The direct-channel Klein bottle amplitude is

$$\begin{aligned} \mathcal{K} = & \frac{1}{8} \left\{ T_{oo} \left[ P_1 P_2 P_3 + P_1 W_2 W_3 + W_1 (-1)^{m_2} P_2 W_3 + (-1)^{n_1} W_1 W_2 (-1)^{m_3} P_3 \right] \right. \\ & \left. + 2 \times 16 T_{go} P_1^{m+1/2} \left( \frac{\eta}{\theta_4} \right)^2 \right\} , \end{aligned} \quad (7.7)$$

the direct-channel annulus amplitude is

$$\begin{aligned} \mathcal{A} = & \frac{1}{8} \left\{ T_{oo} \left[ \frac{N^2}{2} (P_1 + P_1^{m+1/2}) P_2 P_3 + \frac{D_1^2}{4} (P_1 + P_1^{m+1/2}) (W_2 W_3 + W_2^{n+1/2} W_3^{n+1/2}) \right] \right. \\ & \left. + 2F^2 T_{of} (-1)^{m_2} P_2 \left( \frac{2\eta}{\theta_2} \right)^2 + T_{go} N D_1 (P_1^{m+1/4} + P_1^{m+3/4}) \left( \frac{\eta}{\theta_4} \right)^2 \right\} . \end{aligned} \quad (7.8)$$

and finally the Möbius projection is

$$\begin{aligned} \mathcal{M} = & -\frac{1}{8} \left\{ \hat{T}_{oo} \left[ N P_1 P_2 P_3 + D_1 P_1 W_2 W_3 \right] - \hat{T}_{og} (D_1 + N) P_1^{m+1/2} \left( \frac{2\hat{\eta}}{\hat{\theta}_2} \right)^2 \right. \\ & \left. - N \hat{T}_{of} (-1)^{m_2} P_2 \left( \frac{2\hat{\eta}}{\hat{\theta}_2} \right)^2 \right\} . \end{aligned} \quad (7.9)$$

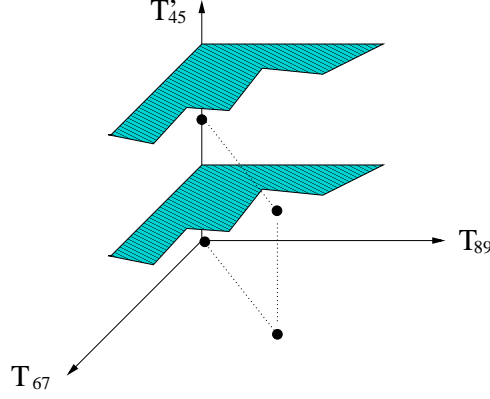


Figure 7.  $D_9$  and  $D5_1$  branes for the  $w_1 p_2 p_3$  model, after  $T_{45}$  duality.

The figure shows, after a  $T_{45}$  duality, the configuration of the  $D9$  branes (now  $D7$  branes, represented as two planes), and of the  $D5_1$  branes (now  $D3$  branes) in the model.

Also in this case, we can parameterize the charges according to

$$N = 2(n + \bar{n}) , \quad F = i(n - \bar{n}) , \quad D_1 = 4d , \quad (7.10)$$

and the tadpole conditions

$$N = D_1 = 32 , \quad (7.11)$$

then require a gauge group

$$U(8)_9 \times SO(8)_{5_1} . \quad (7.12)$$

Again, with a discrete Wilson line on the Möbius strip, one can also obtain a class of models with  $D9$  gauge groups  $SO(n) \times SO(16 - n)$ .

The massless spectrum is again not chiral and has  $N = 2$  supersymmetry on the  $D9$  branes and  $N = 4$  supersymmetry on the  $D5_1$  branes. Moreover, the whole massive spectrum of  $D5_1$  branes has  $N = 2$  supersymmetry. Aside from the gauge multiplets, the spectrum contains pairs of  $N = 2$  hypermultiplets in the representation  $(28, 1)$  from the  $99$  sector. In this model the  $D9$  brane is orthogonal to the  $R_1$  direction, while the  $D5_1$  brane is orthogonal to all three directions used for the breaking. Therefore, the complete local tadpole cancellation in the simultaneous limit  $R_1 \rightarrow 0, R_2, R_3 \rightarrow \infty$  requires a further splitting for the  $D5_1$  brane, with a resulting gauge group  $U(8)_9 \times [SO(4) \times SO(4)]_{5_1}$ .

### 7.3. One momentum shift and two winding shifts

This case corresponds to introducing a momentum shift  $p_2$  along the second torus, and two winding shifts  $w_1$  and  $w_3$  along the other two tori in the table  $\sigma_1$  of eq. (3.1). The resulting models contain  $D9$  and  $D5_1$  branes. The direct-channel Klein bottle amplitude is

$$\begin{aligned} \mathcal{K} = & \frac{1}{8} \left\{ T_{oo} \left[ P_1 P_2 P_3 + P_1 W_2 W_3 + W_1 (-1)^{m_2} P_2 (-1)^{n_3} W_3 + (-1)^{n_1} W_1 W_2 P_3 \right] \right. \\ & \left. + 2 \times 16 T_{go} P_1^{m+1/2} \left( \frac{\eta}{\theta_4} \right)^2 \right\} , \end{aligned} \quad (7.13)$$

the direct-channel annulus amplitude is

$$\begin{aligned} \mathcal{A} = & \frac{1}{8} \left\{ T_{oo} \left[ \frac{N^2}{4} (P_1 + P_1^{m+1/2}) P_2 (P_3 + P_3^{m+1/2}) + \frac{D_1^2}{4} (P_1 + P_1^{m+1/2}) (W_2 + W_2^{n+1/2}) W_3 \right] \right. \\ & \left. + T_{go} N D_1 (P_1^{m+1/4} + P_1^{m+3/4}) \left( \frac{\eta}{\theta_4} \right)^2 \right\} , \end{aligned} \quad (7.14)$$

and finally the Möbius projection is

$$\mathcal{M} = -\frac{1}{8} \left\{ \hat{T}_{oo} \left[ NP_1 P_2 P_3 + D_1 P_1 W_2 W_3 \right] - \hat{T}_{og} (D_1 + N) P_1^{m+1/2} \left( \frac{2\hat{\eta}}{\hat{\theta}_2} \right)^2 \right\}. \quad (7.15)$$

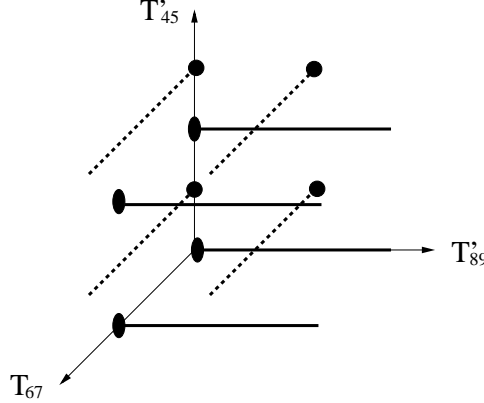


Figure 8.  $D_9$  (dashed) and  $D_{51}$  branes for the  $w_1 p_2 w_3$  model, after  $T_{45}$  and  $T_{89}$  dualities.

Letting  $N = 4n$  and  $D_1 = 4d$ , the tadpole conditions result in the gauge group

$$SO(8)_9 \times SO(8)_{51} \quad . \quad (7.16)$$

In this model the interesting limits are  $R_1, R_3 \rightarrow 0$  and  $R_2 \rightarrow \infty$ . The  $D_9$  branes are orthogonal to the  $R_1, R_3$  directions, while the  $D_{51}$  branes are orthogonal to the  $R_1, R_2$  directions. Thus, complete local tadpole cancellations ask for quadruplets of  $D_9$  and  $D_{51}$  branes, that is indeed the configuration shown in Figure 8. The resulting massless spectrum has  $N = 4$  supersymmetry, both on the  $D_9$  and on the  $D_{51}$  branes, while the massive spectrum has  $N = 2$  supersymmetry on both.

## 8. Freely-acting orbifold models without $D5$ branes

In this Section we provide a description of the remaining classes of shift models, that do not contain  $D5$  branes. As in the previous Sections, for the sake of brevity we only display direct-channel amplitudes.

### 8.1. One momentum shift and two winding shifts

This case corresponds to introducing a momentum shift  $p_1$  along the first torus and two winding shifts  $w_2$  and  $w_3$  along the other tori in the table  $\sigma_2$  of eq. (3.1). The direct-channel Klein bottle amplitude is

$$\mathcal{K} = \frac{1}{8} T_{oo} \left[ P_1 P_2 P_3 + (-1)^{m_1} P_1 W_2 W_3 + W_1 P_2 (-1)^{n_3} W_3 + W_1 (-1)^{n_2} W_2 P_3 \right] , \quad (8.1)$$

the direct-channel annulus amplitude is

$$\mathcal{A} = \frac{1}{8} \left\{ T_{oo} \frac{N^2}{2} P_1 (P_2 P_3 + P_2^{m+1/2} P_3^{m+1/2}) + 2G^2 T_{og} (-1)^{m_1} P_1 \left( \frac{2\eta}{\theta_2} \right)^2 \right\} , \quad (8.2)$$

and finally the Möbius projection is

$$\mathcal{M} = -\frac{1}{8} \left\{ \hat{T}_{oo} N P_1 P_2 P_3 - \hat{T}_{og} N (-1)^{m_1} P_1 \left( \frac{2\hat{\eta}}{\hat{\theta}_2} \right)^2 \right\} . \quad (8.3)$$

Also in this case, we can parameterize the charges according to

$$N = 2(n + \bar{n}) , \quad G = i(n - \bar{n}) , \quad (8.4)$$

and the tadpole conditions

$$N = 32 , \quad G = 0 . \quad (8.5)$$

then require a gauge group

$$U(8)_9 . \quad (8.6)$$

Again, with a discrete Wilson line on the Möbius strip, one can also obtain a class of models with  $D9$  gauge groups  $SO(n) \times SO(16-n)$ . The spectrum is again not chiral and has  $N = 2$  supersymmetry at all mass levels. Aside from the gauge multiplets, the spectrum contains pairs of  $N = 2$  hypermultiplets in the representation  $(28, 1)$  from the 99 sector.

The interesting limits to consider in this case are  $R_1 \rightarrow \infty$  and  $R_2, R_3 \rightarrow 0$ , and the  $D9$  branes are orthogonal to  $R_2$  and  $R_3$ . In the simultaneous  $R_2, R_3 \rightarrow 0$  limit, local tadpole conditions ask for a quadruplet structure, while the  $D9$  branes have actually a

doublet structure. Therefore, the simultaneous local tadpoles ask for a further breaking  $U(8) \rightarrow U(4) \times U(4)$ , while of course the separate limits  $R_2 \rightarrow 0$  (or  $R_3 \rightarrow 0$ ) are not singular.

### 8.2. Three winding shifts

This case corresponds to introducing three winding shifts  $w_1, w_2$  and  $w_3$  along the three tori in the table  $\sigma_1$  of eq. (3.1). The direct-channel Klein bottle amplitude is

$$\mathcal{K} = \frac{1}{8} T_{oo} \left[ P_1 P_2 P_3 + P_1 (-1)^{n_2} W_2 W_3 + W_1 P_2 (-1)^{n_3} W_3 + (-1)^{n_1} W_1 W_2 P_3 \right] , \quad (8.7)$$

the direct-channel annulus amplitude is

$$\mathcal{A} = T_{oo} \frac{N^2}{32} \left[ P_1 P_2 P_3 + P_1 P_2^{m+1/2} P_3^{m+1/2} + P_1^{m+1/2} P_2^{m+1/2} P_3 + P_1^{m+1/2} P_2 P_3^{m+1/2} \right] , \quad (8.8)$$

and finally the Möbius projection is

$$\mathcal{M} = -\frac{1}{8} \hat{T}_{oo} N P_1 P_2 P_3 . \quad (8.9)$$

Letting  $N = 4n$  the tadpole conditions result in the gauge group  $SO(8)_9$  and the full spectrum has  $N = 4$  supersymmetry. The D9 branes are orthogonal to all three directions used for the breaking and the relevant limits to study here are  $R_1, R_2, R_3 \rightarrow 0$ . All local tadpole conditions are automatically satisfied, thanks to the quadruplet structure of branes, with the exception of the simultaneous limit  $R_1, R_2, R_3 \rightarrow 0$ , where new tadpoles ask for the further breaking  $SO(8) \rightarrow SO(4) \times SO(4)$ .

## 9. Conclusions

In this paper we have investigated the open descendants of  $Z_2 \times Z_2$  orbifolds where the orbifold twists are accompanied by various shifts on momentum or winding modes. These shifts result in a generalization [3] of the field-theoretical Scherk-Schwarz mechanism [1] for

(partial) supersymmetry breaking. Therefore, in all our models the partial breaking of supersymmetry may be regarded as spontaneous: extended supersymmetry can be recovered as some radii tend to infinity (zero) in the case of momentum (winding) shifts. We have encountered new instances of the phenomenon noticed in [6, 7]: the massless spectrum of branes orthogonal to the breaking direction is unaffected at tree level, and therefore has typically extended supersymmetry. This, in its turn, makes these models not chiral. We have actually found that in several cases the extended supersymmetry is a property of the full spectrum, not only of the massless modes, as in the asymmetric orbifolds studied in [10]. We have displayed some models with  $N = 2 \rightarrow N = 1$ ,  $N = 4 \rightarrow N = 2$ ,  $N = 4 \rightarrow N = 1$  partial breakings, in addition to the other types, with  $N = 4 \rightarrow N = 0$ ,  $N = 2 \rightarrow N = 0$  and  $N = 4 \rightarrow N = 2$  breakings, discussed in [6, 7]. In particular, in Section 3 we have collected a number of general results on a class of these shifted orbifolds, to which several others may be related via various T-dualities and modifications of the  $\Omega$  projection.

These models display an interesting new geometric feature: since the shifts typically move the fixed points of the orbifolds, branes that would be at fixed points in the unshifted case are actually moved away from them (or, more precisely, from fixed tori, in these  $Z_2 \times Z_2$  models). This gives rise to multiplets of, say,  $m$  image branes, that are typically interchanged by some of the orbifold transformations and are left invariant by others. Thus, in general only some of the orbifold projections affect the partition function, and as a result the massless modes, and often even the massive ones, have generically extended supersymmetry. The rank of the corresponding gauge groups is also affected, and is reduced to  $16/m$ . This phenomenon of brane displacement, discussed for the supersymmetric  $T^4/Z_2$  model in [21], presents some analogies with the corresponding one induced by quantized  $NS - NS$  antisymmetric tensor field backgrounds in the compact space [11].

We have also seen how, in general, the shifts make some of tadpole terms in the Klein bottle massive, eliminating the corresponding D5 branes, and we have presented explicit

realizations of models with two, one and no D5 branes in the spectrum. All these models are not chiral, a feature that can be traced to the lack of some of the breaking terms for  $ND$  or  $D_i D_j$  strings or, equivalently, to the multiplet structure of the branes.

We have provided an M-theory interpretation of some of the models, that can be related to Scherk-Schwarz deformations along the eleventh dimension of M-theory compactified on an appropriate manifold [23, 6, 7]. In this case, once a local tadpole cancellation condition is fulfilled in the coordinate used for the breaking, two sets of branes orthogonal to the breaking direction may be interpreted as a pair of Horava-Witten walls.

These models provide examples of partial supersymmetry breaking where gravity can be decoupled from the brane dynamics. Thus, it would be interesting to study in detail the structure of the effective field theory and to compare it with the known realizations of partial supersymmetry breaking [24]. Moreover, the issue of radiative corrections is quite interesting, and was partly addressed, for the gauge couplings, in [25]. For branes parallel to the breaking direction, the corrections have a logarithmic dependence on the corresponding radius, while for branes orthogonal to the breaking coordinate, in models with local tadpole cancellation, they are exponentially small, in agreement with the considerations presented in [26].

## Acknowledgments

We are grateful to C. Angelantonj, K. Ray, and in particular to E. Kiritsis and Ya.S. Stanev for useful discussions. The work of G.D. was supported in part by EEC TMR contract ERBFMRX-CT96-0090, while the work of A.S. was supported in part by CNRS. G.D. and A.S. would like to thank the Centre the Physique Théorique of the Ecole Polytechnique for the kind hospitality extended to them during the course of this research.

## References

- [1] J. Scherk and J.H. Schwarz, *Nucl. Phys.* **B153** (1979) 61, *Phys. Lett.* **B82** (1979) 60; R. Rohm, *Nucl. Phys.* **B237** (1984) 553; P. Fayet, *Phys. Lett.* **B159** (1985) 121, *Nucl. Phys.* **B263** (1986) 649.
- [2] C. Kounnas and M. Petraki, *Nucl. Phys.* **B310** (1988) 355; S. Ferrara, C. Kounnas, M. Petraki and F. Zwirner, *Nucl. Phys.* **B318** (1989) 75; C. Kounnas and B. Rostand, *Nucl. Phys.* **B341** (1990) 641; I. Antoniadis, *Phys. Lett.* **B246** (1990) 377; I. Antoniadis and C. Kounnas, *Phys. Lett.* **B261** (1991) 369.
- [3] E. Kiritsis and C. Kounnas, *Nucl. Phys.* **B503** (1997) 117.
- [4] C. Vafa and E. Witten, *Nucl. Phys. Proc. Suppl.* **46** (1996) 225.
- [5] A. Sagnotti, in: Cargèse '87, Non-Perturbative Quantum Field Theory, eds. G. Mack et al. (Pergamon Press, Oxford, 1988) p. 521; G. Pradisi and A. Sagnotti, *Phys. Lett.* **B216** (1989) 59; M. Bianchi and A. Sagnotti, *Phys. Lett.* **B247** (1990) 517, *Nucl. Phys.* **B361** (1991) 519.
- [6] I. Antoniadis, E. Dudas and A. Sagnotti, *Nucl. Phys.* **B544** (1999) 469.
- [7] I. Antoniadis, G. D'Appollonio, E. Dudas and A. Sagnotti, hep-th/9812118, *Nucl. Phys.* **B553** (1999) 133.
- [8] Z. Kakushadze and S.-H.H. Tye, *Nucl. Phys.* **B548** (1999) 180.
- [9] S. Kachru and E. Silverstein, JHEP 11 (1998) 001, hep-th/9810129; J. Harvey, *Phys. Rev.* **D59** (1999) 26002.

- [10] R. Blumenhagen and L. Görlich, hep-th/9812158;  
C. Angelantonj, I. Antoniadis and K. Foerger, hep-th/9904092.
- [11] M. Bianchi, G. Pradisi and A. Sagnotti, *Nucl. Phys.* **B376** (1992) 365;  
M. Bianchi, *Nucl. Phys.* **B528** (1998) 73;  
E. Witten, *J. High Energy Phys.* **02** (1998) 006;  
Z. Kakushadze, G. Shiu and S.-H.H. Tye, *Phys. Rev.* **D58** (1998) 086001;  
M. Bianchi, E. Gava, F. Morales and K.S. Narain, hep-th/9811013.
- [12] I. Antoniadis, E. Dudas and A. Sagnotti, in preparation.
- [13] C. Vafa, *Nucl. Phys.* **B273** (1986) 592;  
C. Vafa and E. Witten, *J. Geom. Phys.* **B15** (1995) 189.
- [14] J. Polchinski and E. Witten, *Nucl. Phys.* **B460** (1996) 525.
- [15] M. Berkooz and R.G. Leigh, *Nucl. Phys.* **B483** (1997) 187.
- [16] M. Bianchi, Ph.D. Thesis, preprint ROM2F-92/13;  
A. Sagnotti, hep-th/9302099.
- [17] R. Gopakumar and S. Mukhi, *Nucl. Phys.* **B479** (1996) 260.
- [18] A. Dabolkhar and J. Park, *Nucl. Phys.* **B472** (1996) 207,  
*Nucl. Phys.* **B477** (1996) 701.
- [19] C. Angelantonj, M. Bianchi, G. Pradisi, A. Sagnotti and Ya.S. Stanev,  
*Phys. Lett.* **B387** (1996) 743.
- [20] M. Bianchi and A. Sagnotti, in [5].
- [21] E. Gimon and J. Polchinski, hep-th/9601038.
- [22] P. Horava and E. Witten, *Nucl. Phys.* **B460** (1996) 506, **B475** (1996) 94.

- [23] I. Antoniadis and M. Quiros, *Phys. Lett.* **B392** (1997) 61;  
E. Dudas and C. Grojean, *Nucl. Phys.* **B507** (1997) 553;  
I. Antoniadis and M. Quiros, *Nucl. Phys.* **B505** (1997) 109,  
*Phys. Lett.* **B416** (1998) 327;  
E. Dudas, *Phys. Lett.* **B416** (1998) 309.
- [24] I. Antoniadis, H. Partouche and T.R. Taylor, *Phys. Lett.* **B372** (1996) 83;  
S. Ferrara, L. Girardello and M. Petrati, *Phys. Lett.* **B366** (1996) 155;  
J. Bagger and A. Galperin, *Phys. Lett.* **B412** (1997) 296, *Phys. Rev.* **D55** (1997) 1091.
- [25] I. Antoniadis, C. Bachas and E. Dudas, hep-th/9906039.
- [26] I. Antoniadis and C. Bachas, *Phys. Lett.* **B450** (1999) 83.